united nations
educational, scientific
and cultural
organization

international atomic
energy agency

the
**abdus salam**
international centre for theoretical physics

**SMR 1232 - 30**

## XII WORKSHOP ON
## STRONGLY CORRELATED ELECTRON SYSTEMS

**17 - 28 July 2000**

# *MAGNETIC EXCITON MEDIATED SUPERCONDUCTIVITY IN $UPd_2Al_3$*

N.K. SATO
Department of Physics
Nagoya University
Nagoya, Japan

# Magnetic exciton mediated superconductivity in $UPd_2Al_3$

N. K. Sato (佐藤 憲昭)
Department of Physics, Nagoya University, Nagoya, Japan

Collaborators

N. Aso (University of Tokyo)
K. Miyake (Osaka University)
R. Shiina (Tokyo Metropolitan University)
P. Thalmeier (MPI)
G. Varelogiannis (MPI)
C. Geibel (MPI)
F. Steglich (MPI)
P. Fulde (MPI)
T. Komatsubara (Tohoku University)

Coexistence of AF ($T_N$ = 14.3 K) and SC ($T_C$ ~ 2 K), both of which are carried by 5f electrons.

Strong repulsive Coulomb interaction leads to (localized) magnetism.

Superconductivity needs an attractive interaction between quasiparticles.

Is the coexistence of AF and SC possible?

Typical example: **$RERh_4B_4$**
**$REMo_6S_8$ (Chevrel)**

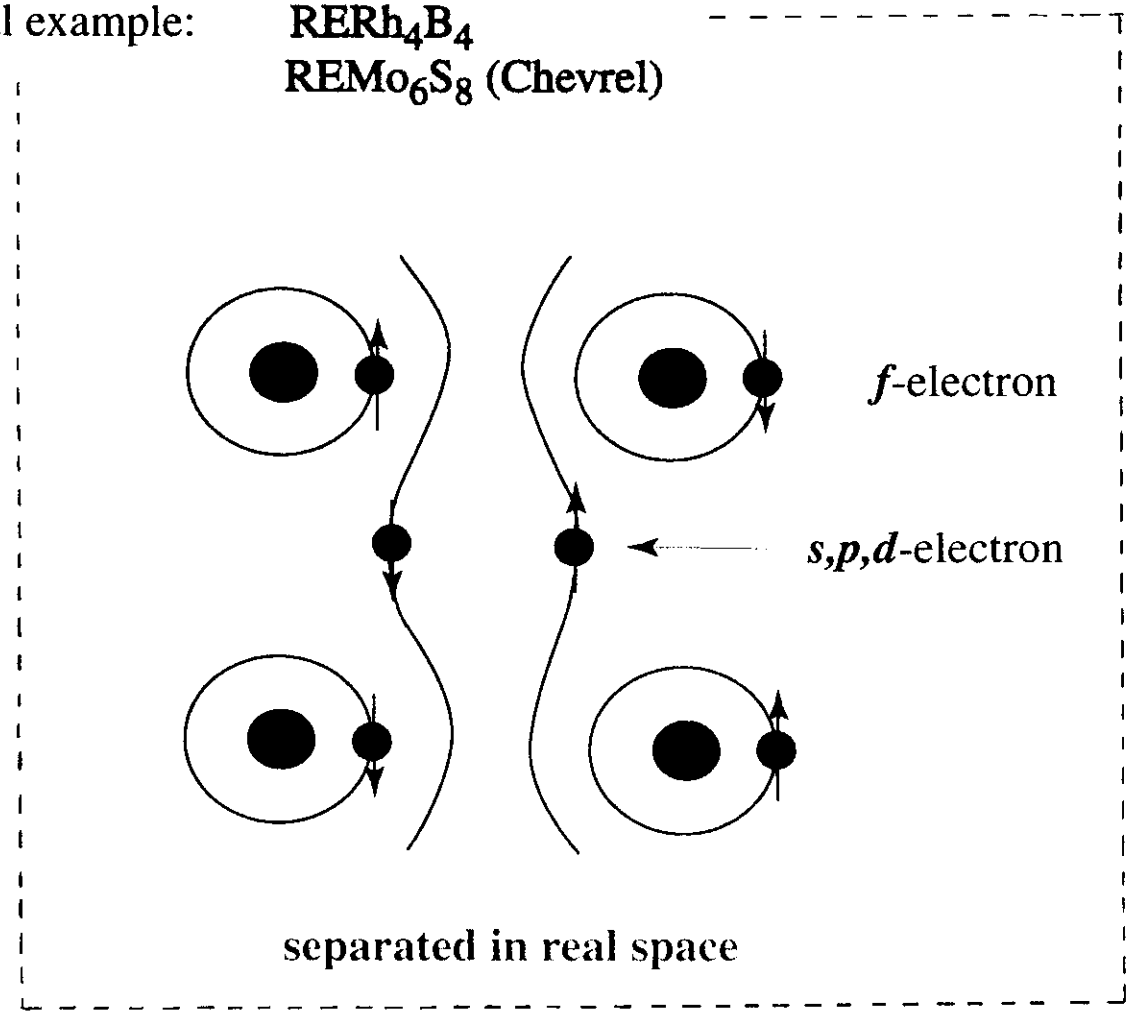


Localized 4*f* electrons of RE are responsible for magnetism, and *s, p, d* electrons carrying SC current have no amplitude on RE.

Outline

1. Introduction

    Magnetic & superconducting properties

2. Experimental results of inelastic neutron scattering

3. Model & analysis

(4. $UNi_2Al_3$)

5. Summary

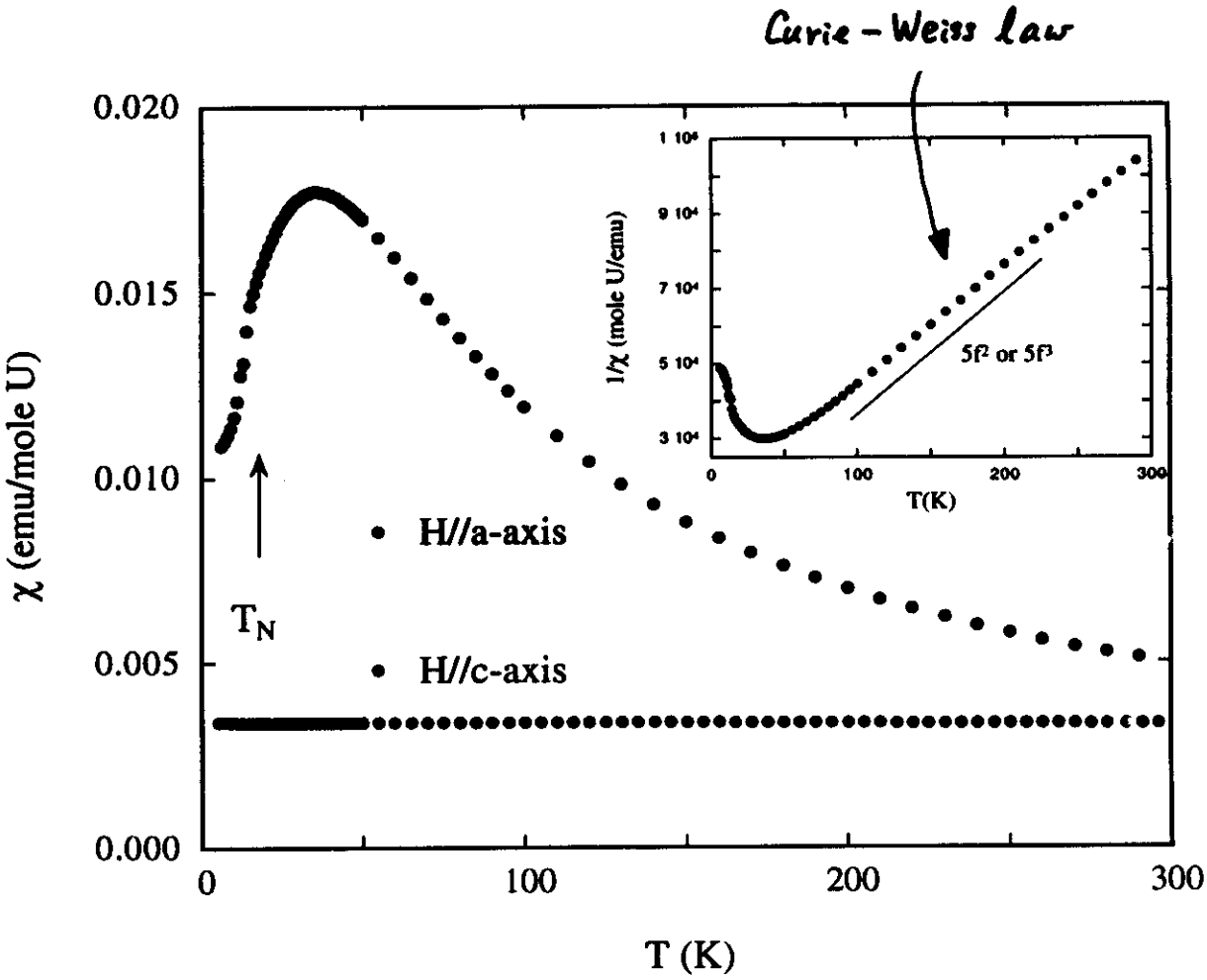


large anisotropic temperature dependence

↓

crystal field effect

↓

localized moment

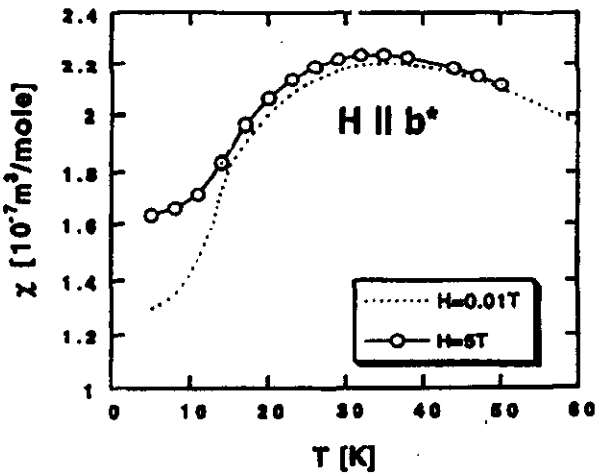


**Figure 1.** DC magnetic susceptibility versus temperature as measured on the same crystal as used for the neutron studies measured in applied fields of 5 T (O) and 0.01 T (----).

experiment. These susceptibility measurements were performed on the SQUID magnetometer at the Centre d'Etudes Nucléaires, Grenoble collecting 15 different temperatures from 5 to 50 K. Measurements of the susceptibility at $H = 0.01$ T (performed at Sendai) are shown also for this direction in figure 1. The susceptibility is slightly non-linear with field; for example $H = 0.01$ T the maximum value is $2.2 \times 10^{-7}$ m$^3$ mol$^{-1}$, whereas at 5 T we find this has increased to $2.26 \times 10^{-7}$ m$^3$ mol$^{-1}$.

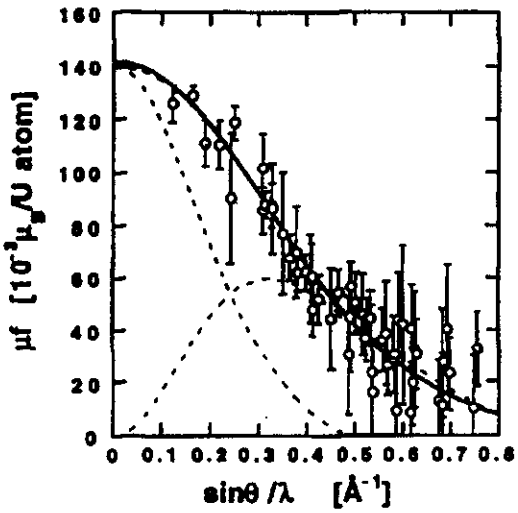


**Figure 2.** Magnetic scattering amplitudes as measured at 36 K in an applied field of 5 T and plotted versus $(\sin\theta)/\lambda$ assuming that the total response is located at the uranium site. The best fits to the dipole approximation for $U^{4+}$ and $U^{3+}$ are shown as full and bold broken curves respectively. They are almost indistinguishable. The broken curves correspond to the functions $\langle j_0 \rangle$ and $\langle j_2 \rangle$ for $U^{3+}$ used in the fit (see Freeman *et al* (1976)).

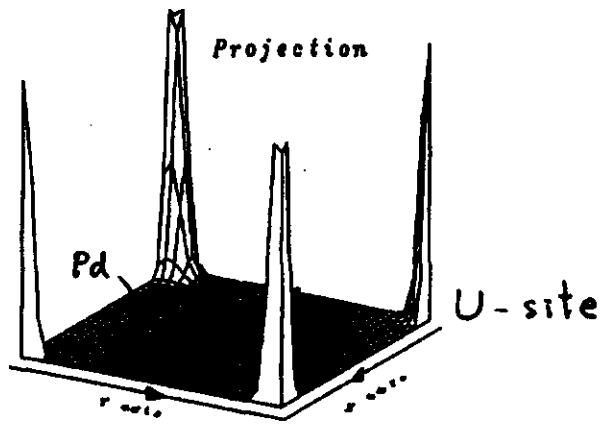


**Figure 3.** Maximum-entropy reconstruction of the magnetization density projected on the basal plane of the hexagonal $UPd_2Al_3$ structure. The high values are associated with the density at the uranium sites; the arrows indicate the positions of the palladium sites. The $x$ axis is parallel to the hexagonal $a$ axis, and the $y$ axis is perpendicular to it.

magnetic form factor

$\vec{Q}_0 = (0, 0, \frac{1}{2})$ , $\vec{\mu}_a \approx 0.85\ \mu_B$

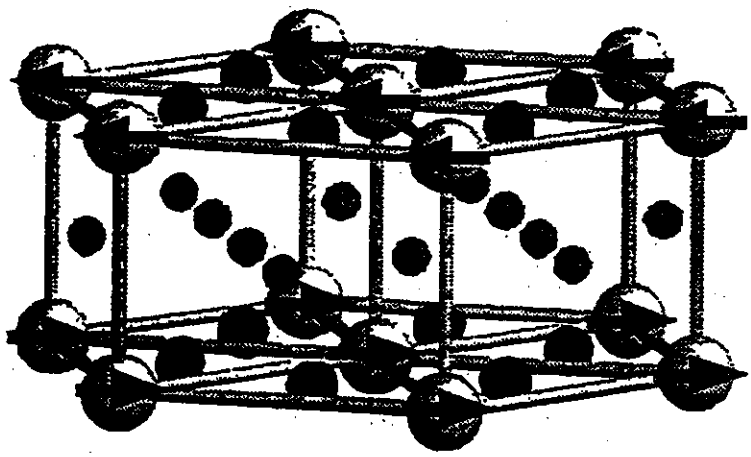

FIG. 1. Crystal structure of $UPd_2Al_3$ (hexagonal, $PrNi_2Al_3$ type). Large spheres at the corners are U atoms with the magnetic moments denoted by arrows, and they are surrounded by Pd atoms in the hexagonal basal plane. Small spheres indicate Al atoms located between the planes.

($PrNi_2Al_3$ type, $P6/mmm$, $a$=5.37 Å, $c$=4.18 Å).

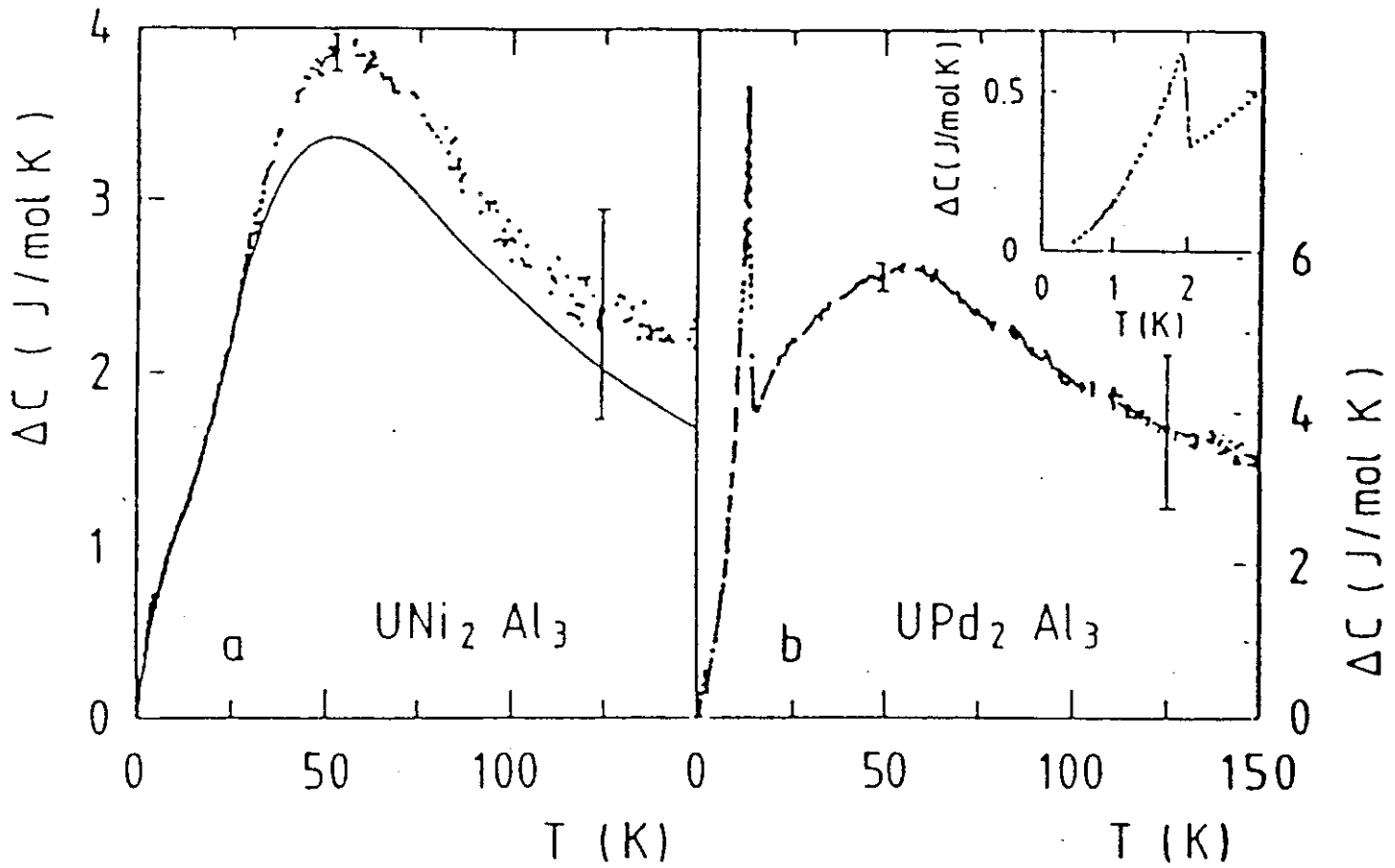


**FIGURE 4**

$\Delta C = C(UT_2Al_3)\text{-}C(ThT_2Al_3)$ vs T for T = Ni (a) and T = Pd (b). Solid curve in (a) represents Bethe-Ansatz result for spin 1/2 single-ion Kondo effect ($T_K$ = 48K) and a doublet-singlet CF splitting of $k_B \cdot 125K$. Inset in (b) shows superconducting transition for $UPd_2Al_3$ (Ref.9).

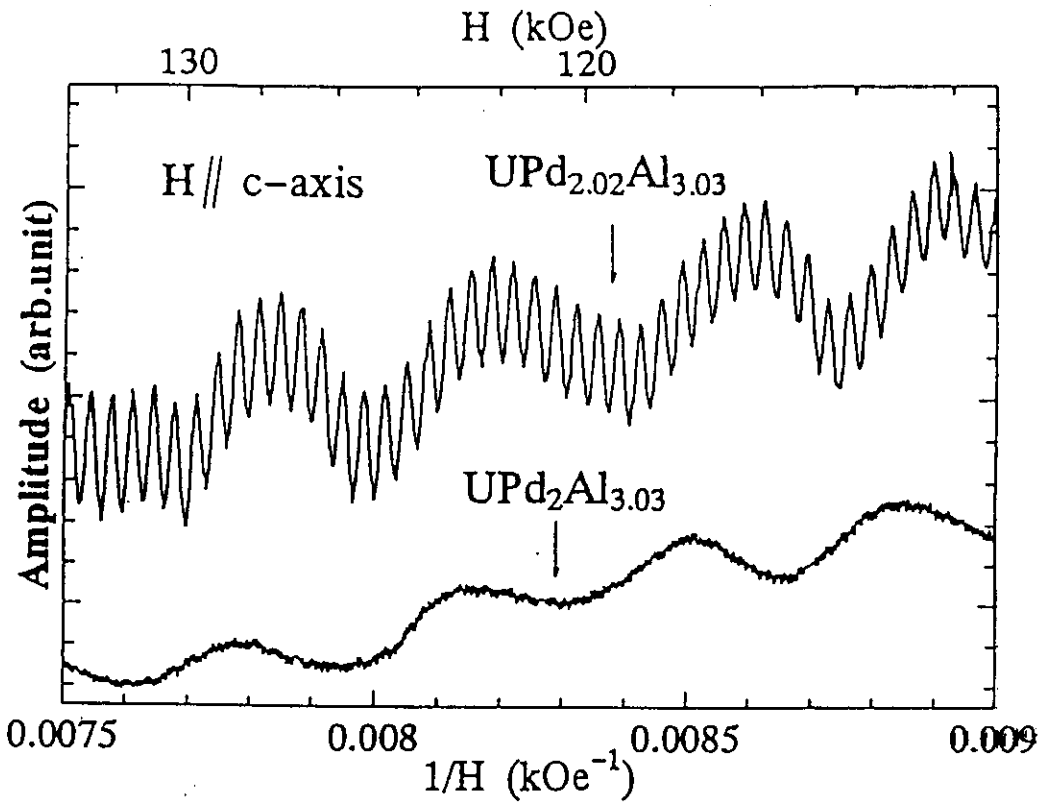


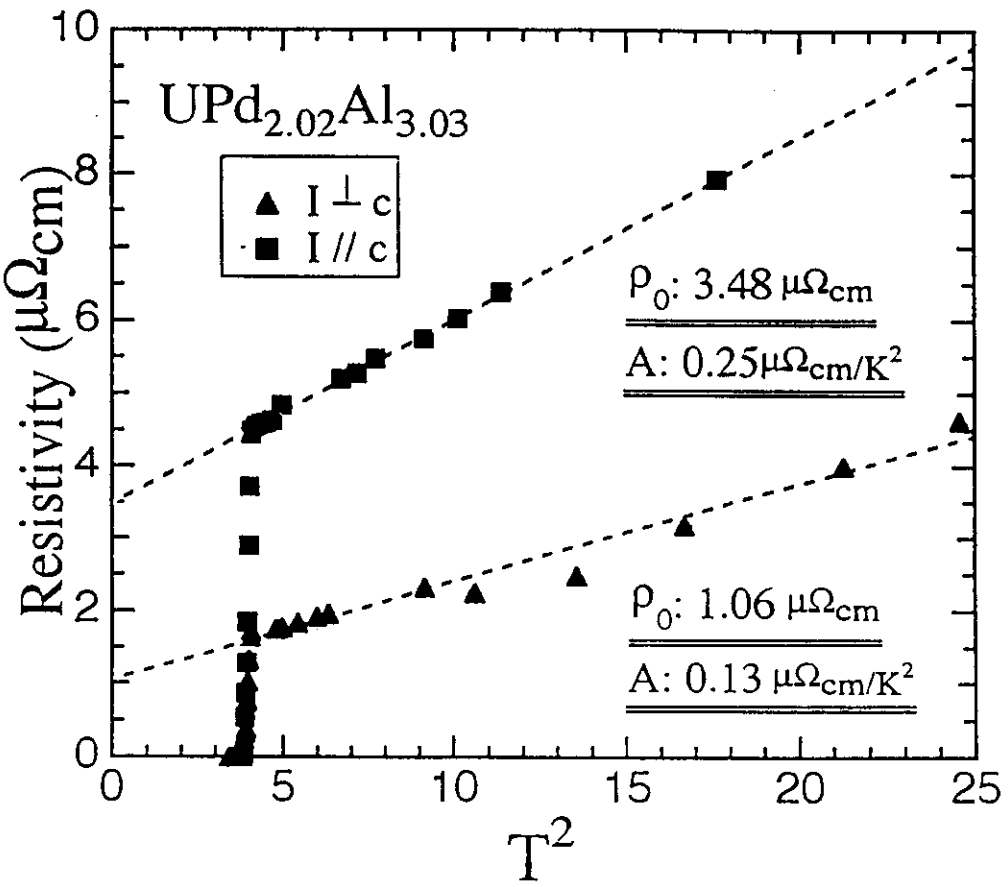


図3-2-4 $UPd_{2.02}Al_{3.03}$の残留抵抗の異方性。 Y. Inada, Thesis (1994) (Tohoku Univ.)

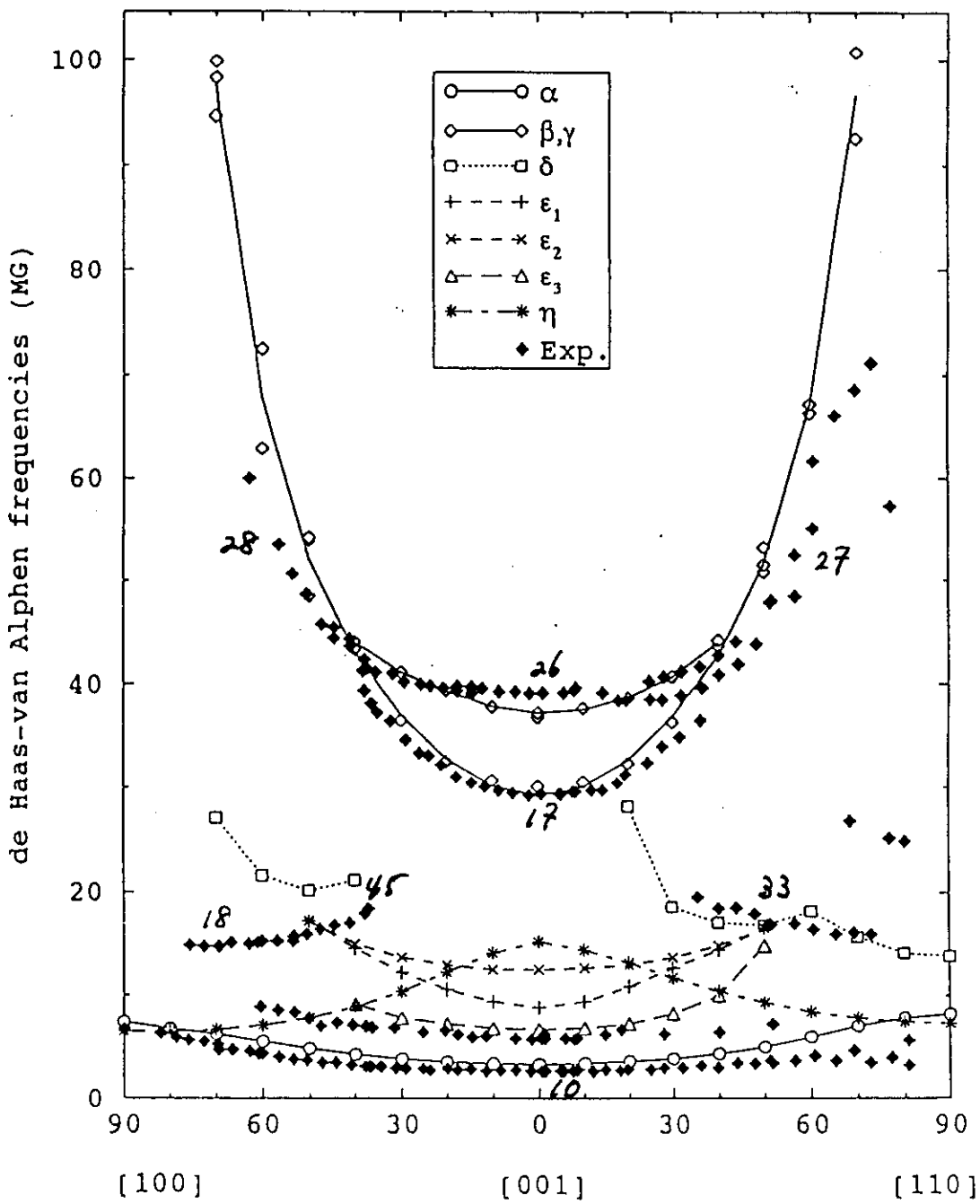


large cyclotron mass.

=

direct evidence for heavy quasiparticles !

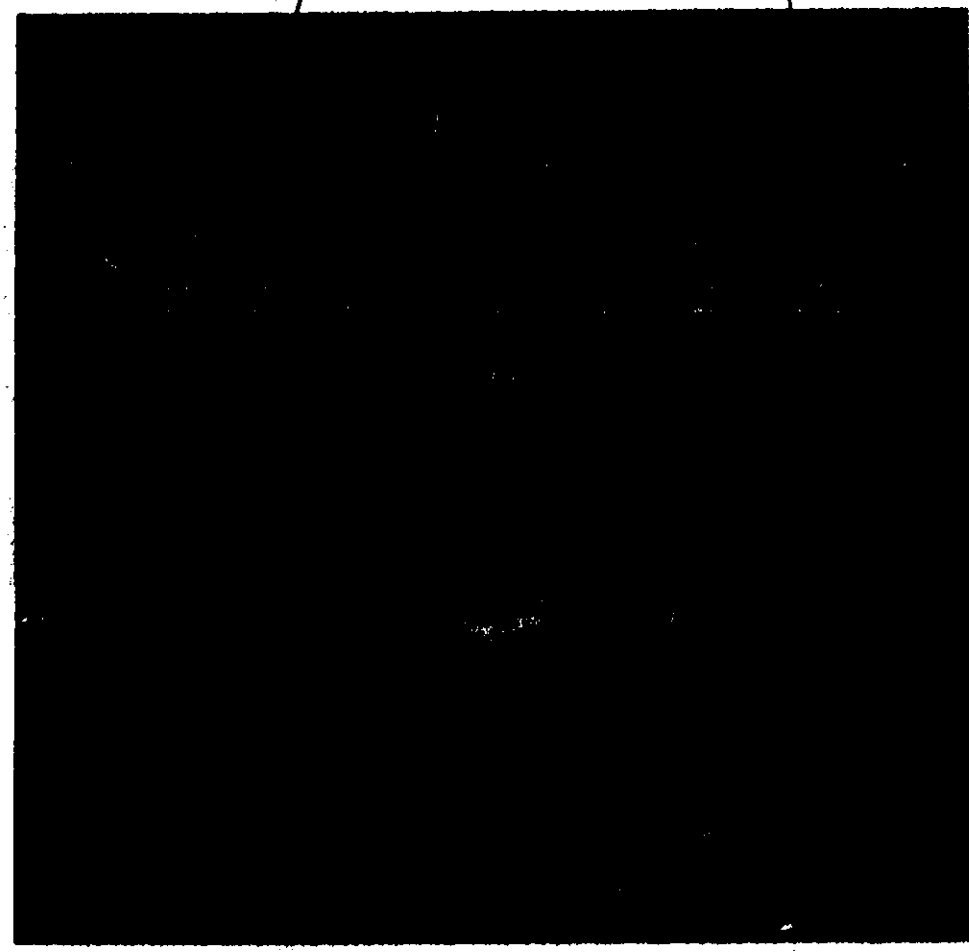

Figure 6. Fermi surfaces as in figure 5. The colours shown give the amount of 5f angular momentum character on each sheet of the Fermi surface.

of the surface. We stress the distinction of the two largest sheets of the FS: 'party hat' and 'column'. The latter is an almost pure 5f sheet in contrast to the former which is formed by strongly hybridized states. Again, the extent of the hybridization is very different in different parts of the surface.

This result lends considerable weight to the assumption about different types of state at the Fermi level made in [4, 5, 6]. Since one of the experimental distinctions is the anisotropy of the magnetic susceptibility we extend the comparison by calculating the magnetic response of the bands forming different sheets of the FS to a magnetic field applied, respectively, parallel to the $y$ and the $z$ axes (figure 1) as described in the previous section. The value of the field is chosen so that $\mu_B B$ equals 1 mRyd. The results of the calculation of the susceptibility are collected together in table 1. Note that in the absence of the field the collinear antiferromagnetic structure leads to double degeneracy of all energy bands and therefore of all sheets of the FS. The external magnetic field lowers the symmetry and lifts the degeneracy of the bands. As a result, the two degenerate bands

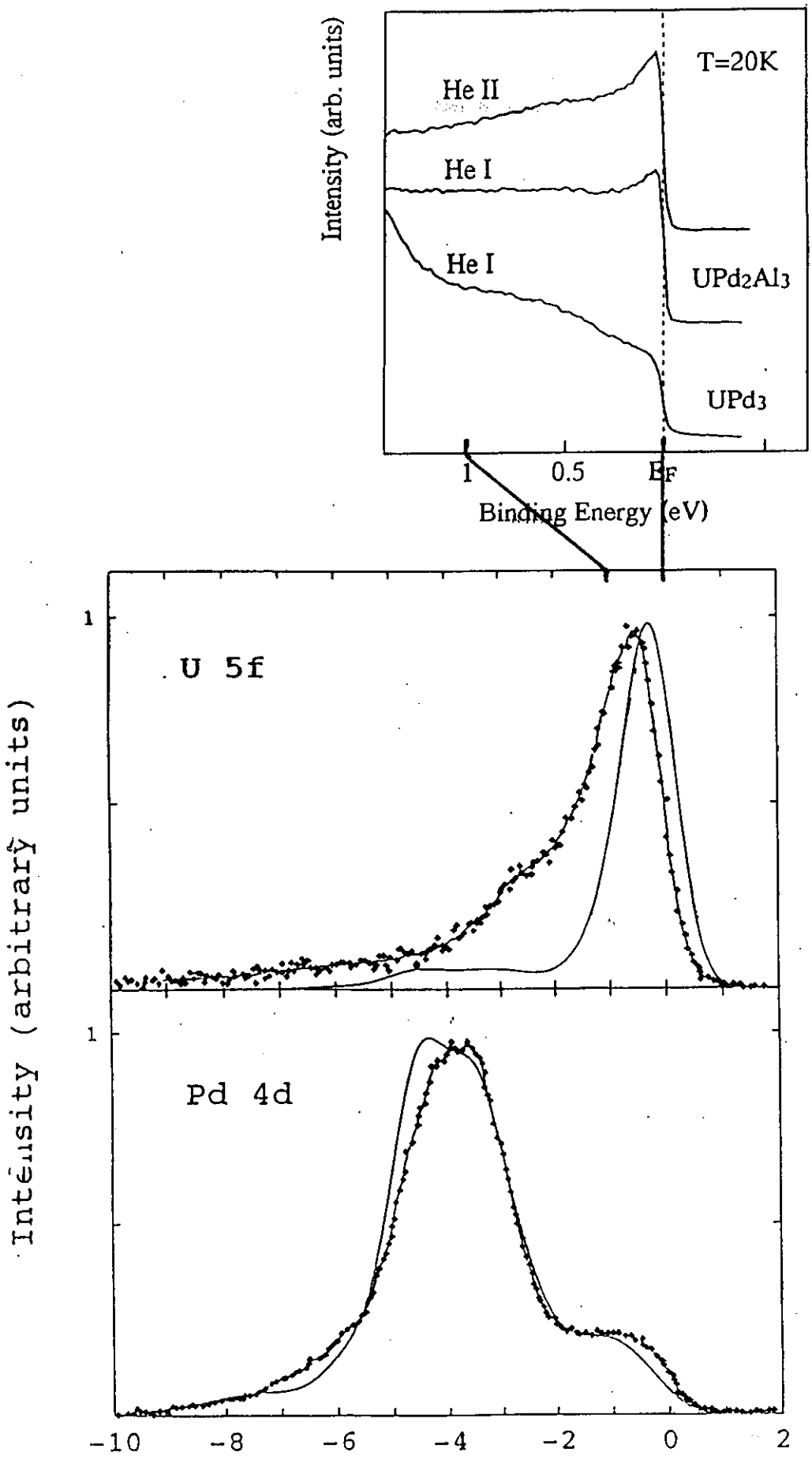
Intensity (arb. units)
T=20K
He II
He I
He I
UPd2Al3
UPd3
1
0.5
EF
Binding Energy (eV)
U 5f
Pd 4d
Intensity (arbitrary units)
-10
-8
-6
-4
-2
0
2
Energy (eV)

Magnetism

carried by $5f$ electrons of uranium ions

Key point

two-component nature of $5f$ electrons

localized vs itinerant

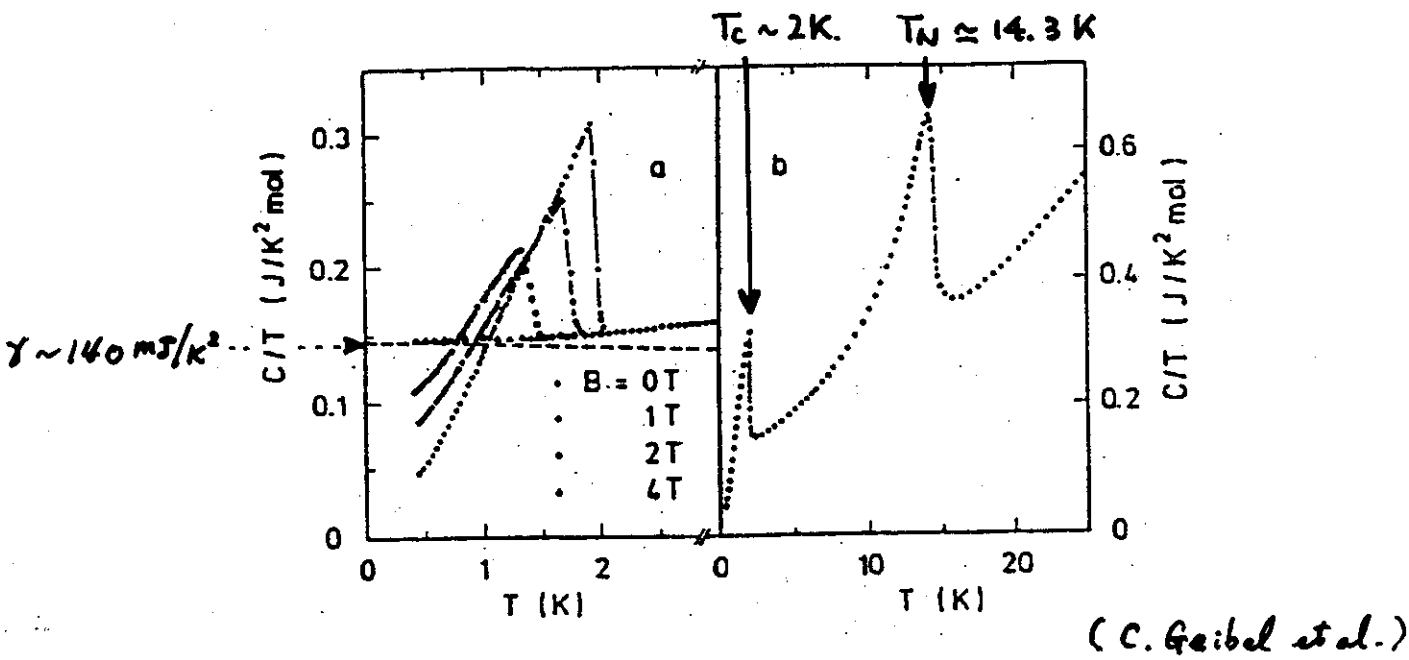


図２．多結晶の比熱の温度変化[1)]

μSR

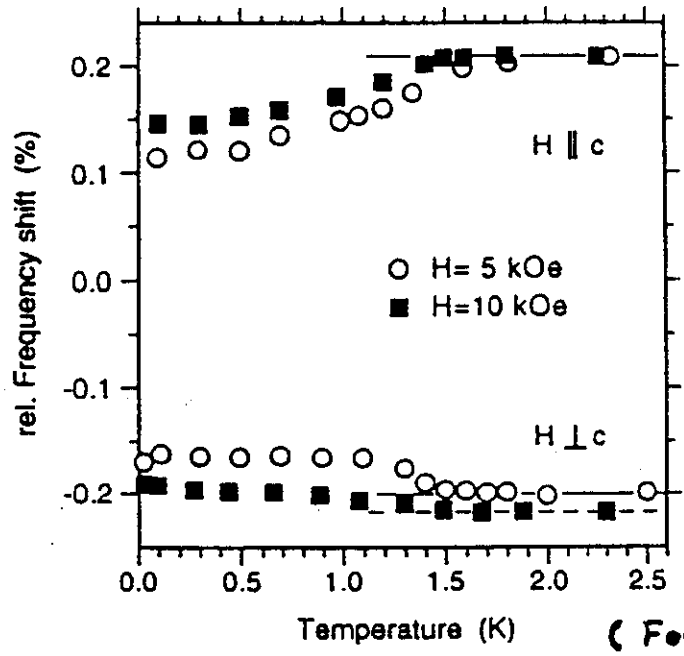


( Fogerhom et al.)

NMR

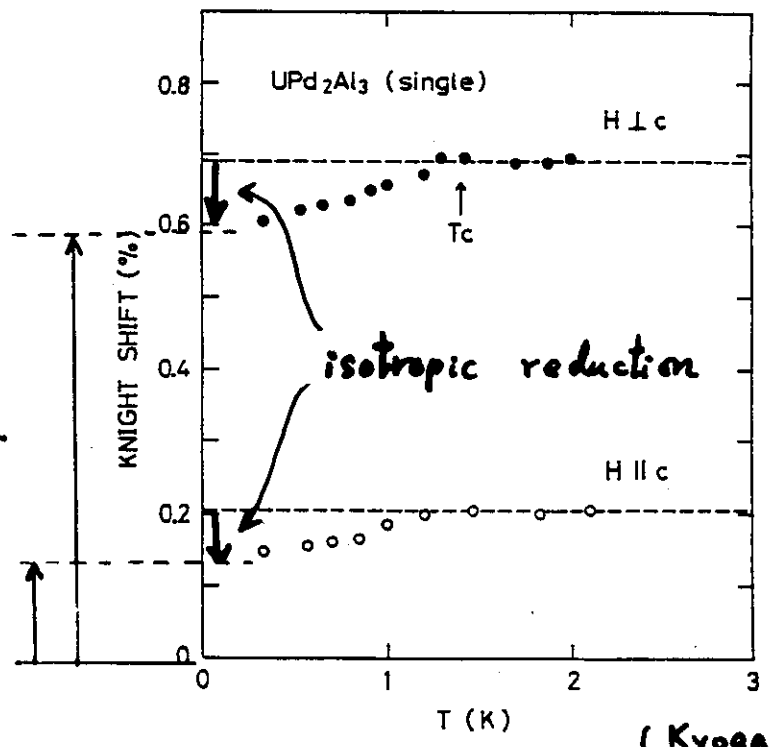


anisotropic residual part

( Kyogaku et al.)

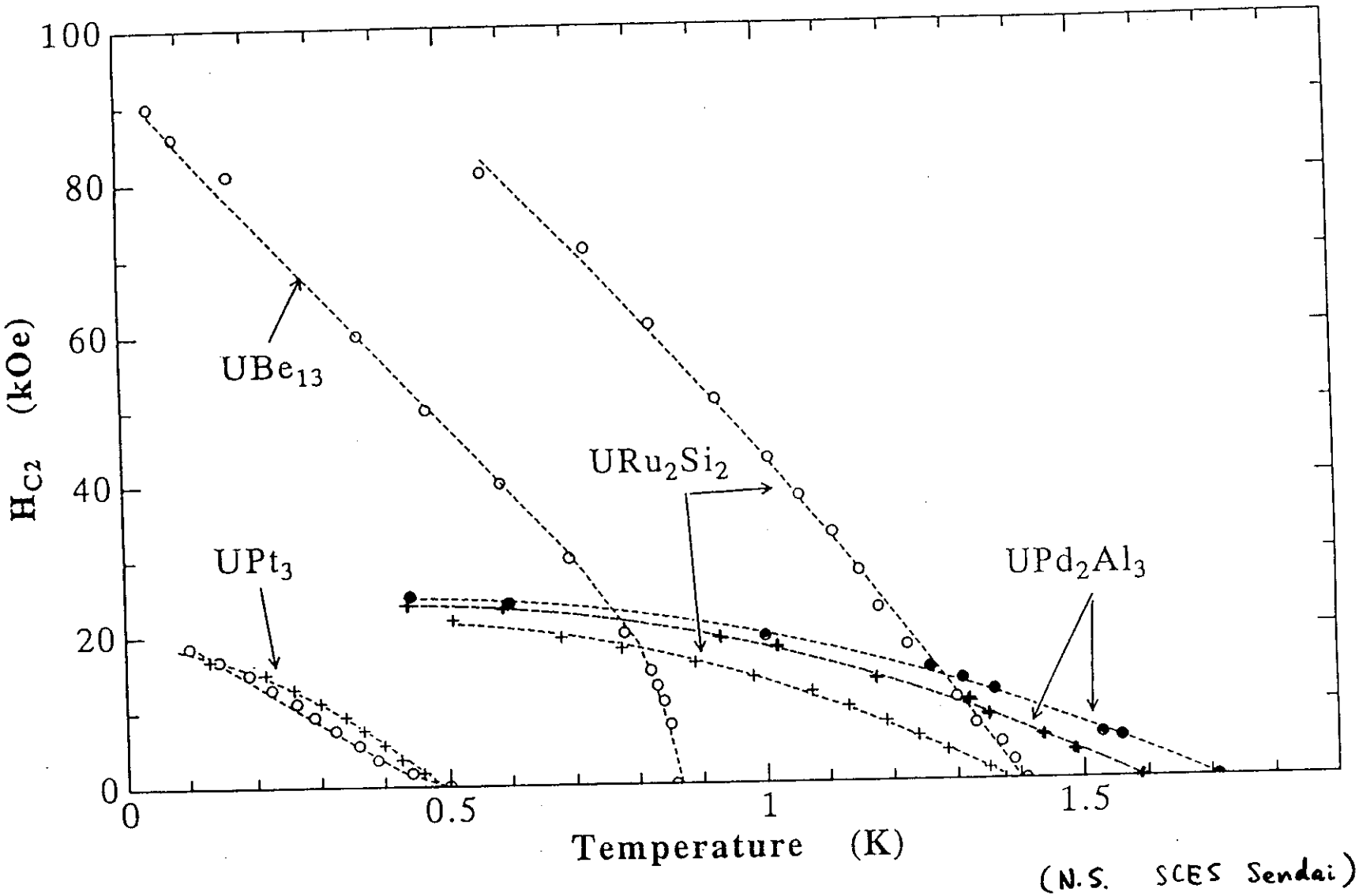


(N.S. SCES Sendai)

$C \propto T^{2.5}$

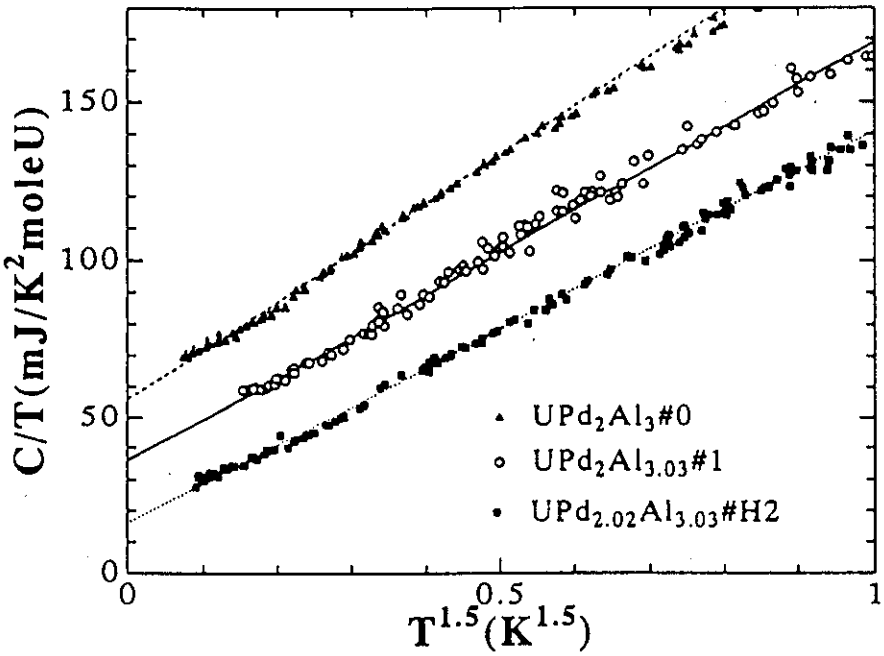


$C \propto T^{3}$

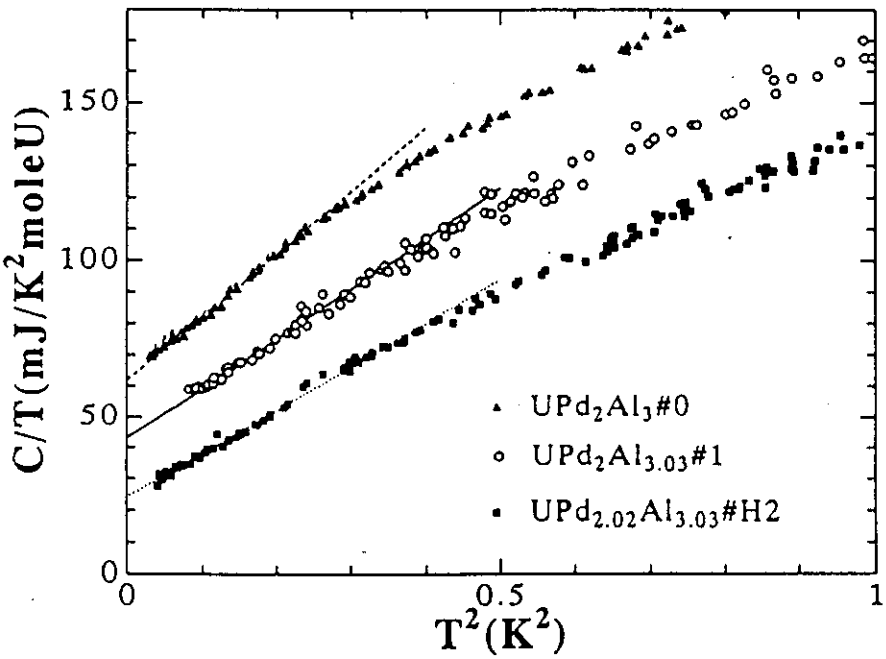


( Sakon et al. )

cf. $\frac{1}{T_1} \propto T^3$

Superconductivity (SC):

Itinerant component of 5*f* electrons

forms Fermi liquids with the heavy effective cyclotron mass,

and condenses into SC.

Key point:

5*f* electrons are responsible for both AF and SC.

Correlation between AF and SC ?

Does AF destroy or assist SC ?

ELSEVIER

Physica B 199&200 (1994) 151–153

PHYSICA B

# Magnetic fluctuations and the superconducting transition in the heavy-fermion material $UPd_2Al_3$

T. Petersen[a,b,*], T.E. Mason[a,b], G. Aeppli[c], A.P. Ramirez[c], E. Bucher[c], R.N. Kleiman[c]

[a] *Department of Solid State Physics, Riso National Laboratory, 4000 Roskilde, Denmark*
[b] *Department of Physics, University of Toronto, Toronto, Ontario, M5S 1A7 Canada*
[c] *AT&T Bell Labs, 600 Mountain Ave., Murray Hill, NJ, USA*

**Abstract**

Inelastic neutron scattering has been performed on single crystals of the heavy-fermion superconductor $UPd_2Al_3$. The antiferromagnetically ordered state is characterized by an acoustic spin wave mode with no gap. The low-frequency magnitude excitations are unaffected by the transition to a superconducting state despite coupling to the conduction electrons as evidenced by the significant damping.

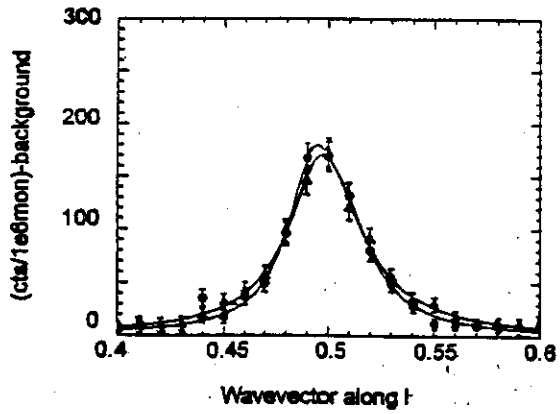


Fig. 3. Constant $\hbar\omega_f$ scans at $\hbar\omega_f = 0.3$ meV, $T = 0.4$ K and 1.8 K.

No temperature dependence below and above $T_c$ !?

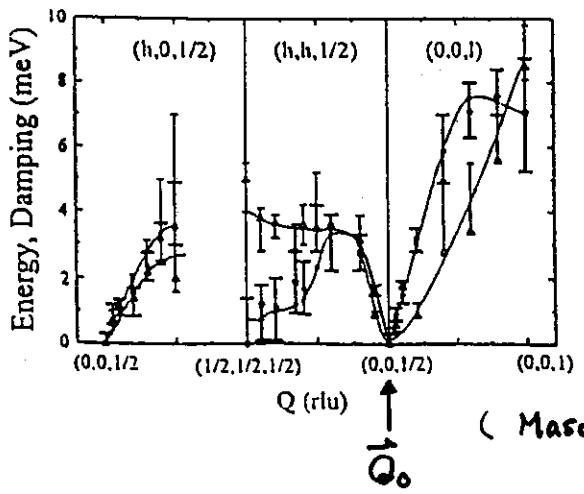


( Mason et al.)

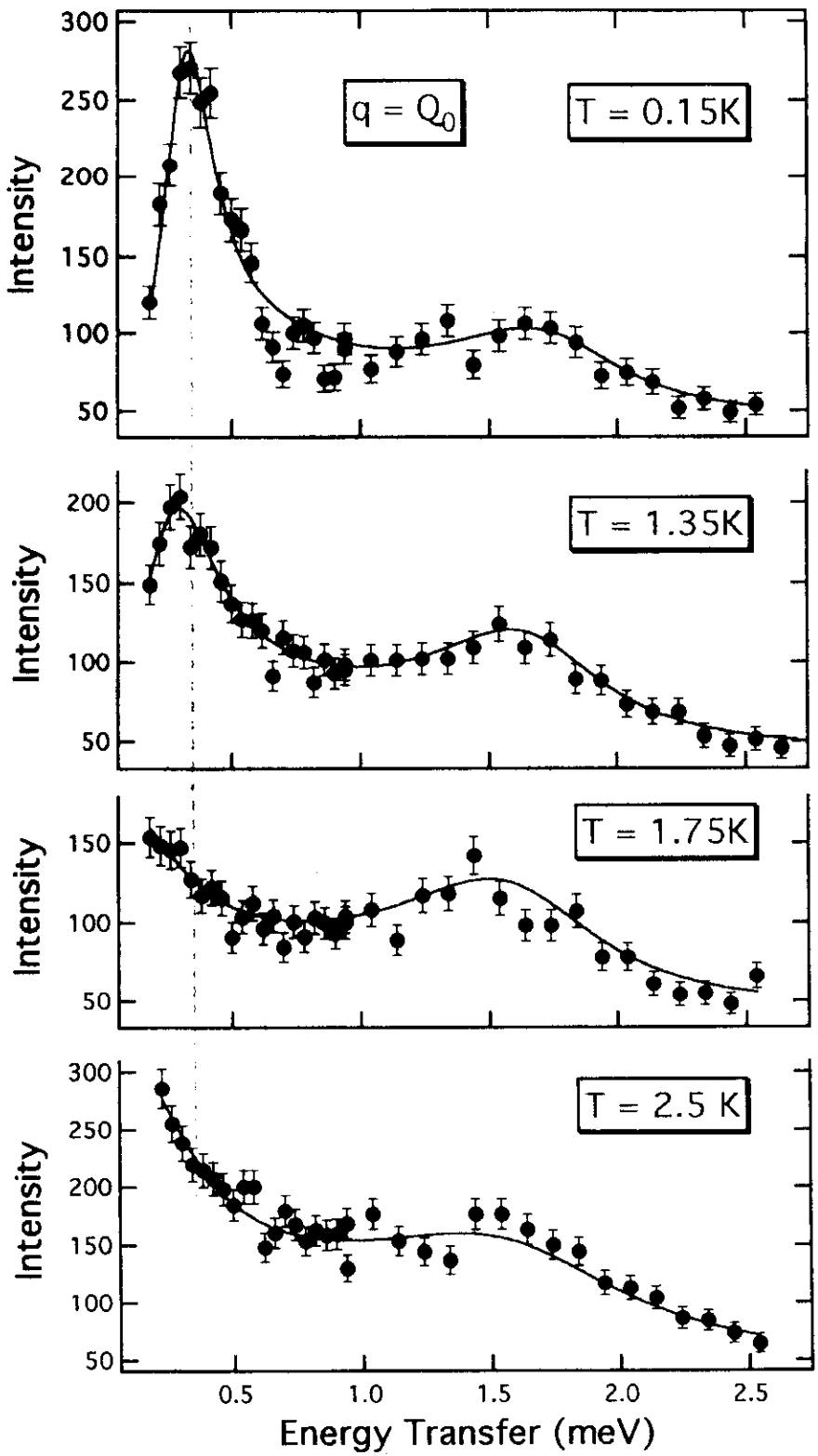
q = Q0
T = 0.15K
T = 1.35K
T = 1.75K
T = 2.5 K
Intensity
Energy Transfer (meV)
300
250
200
150
100
50
0.5
1.0
1.5
2.0
2.5

$T \sim T_c$

reciprocal lattice vector

$Q = (2\pi/c)(0,0,1)$

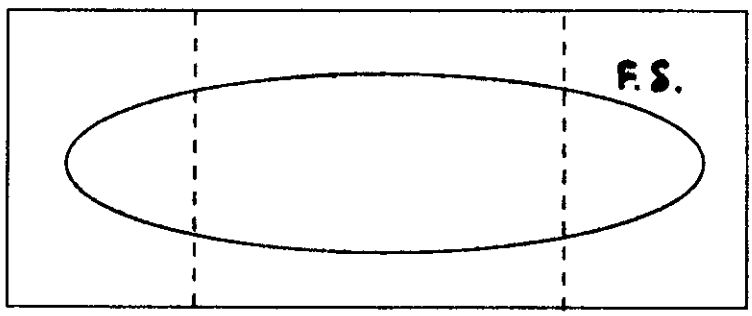


$T > T_N$

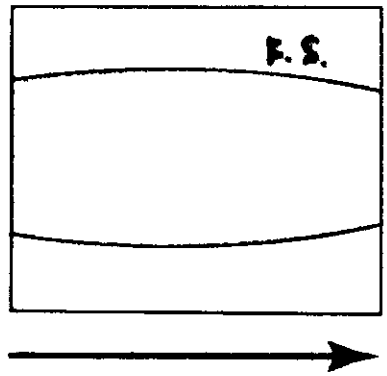


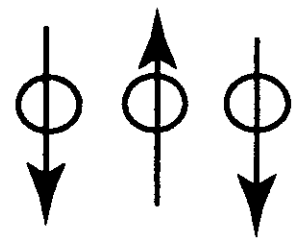

$T < T_N$

$Q_0 = (2\pi/c)(0,0,1/2)$

is equivalent to $q = 0$ for itinerant electrons.

pair breaking ;

$$\chi(q,\omega) = \sum_k \left(1 - \frac{\xi(k+q)\xi(k) + \Delta(k+q)\Delta(k)}{E(k+q)E(k)}\right) \frac{1 - f(E(k+q)) - f(E(k))}{\omega - (E(k+q) + E(k)) + i\Gamma}$$

**coherence factor**

where $E(k)^2 = \xi(k)^2 + \Delta(k)^2$ .

If $\Delta(q + Q_0) = \Delta(q)$ , then the coherence factor is vanishing.

The existence of the low energy response implies

$$\Delta(q + Q_0) = -\Delta(q).$$

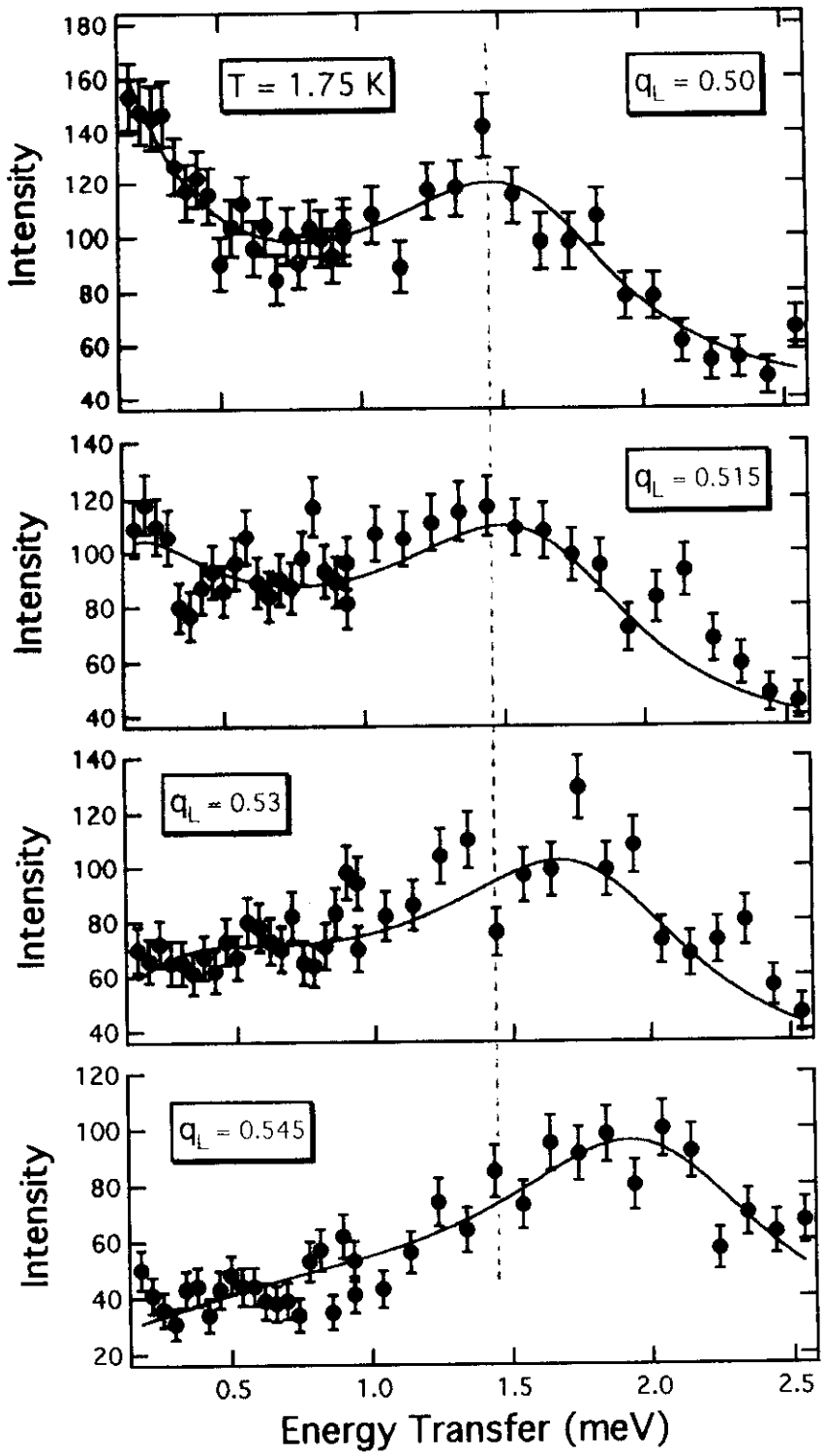
T = 1.75 K
$q_L$ = 0.50
$q_L$ = 0.515
$q_L$ = 0.53
$q_L$ = 0.545
Intensity
Energy Transfer (meV)

Basic assumption

$5f^{-3} \longrightarrow 5f^{2} + 5f^{1}$

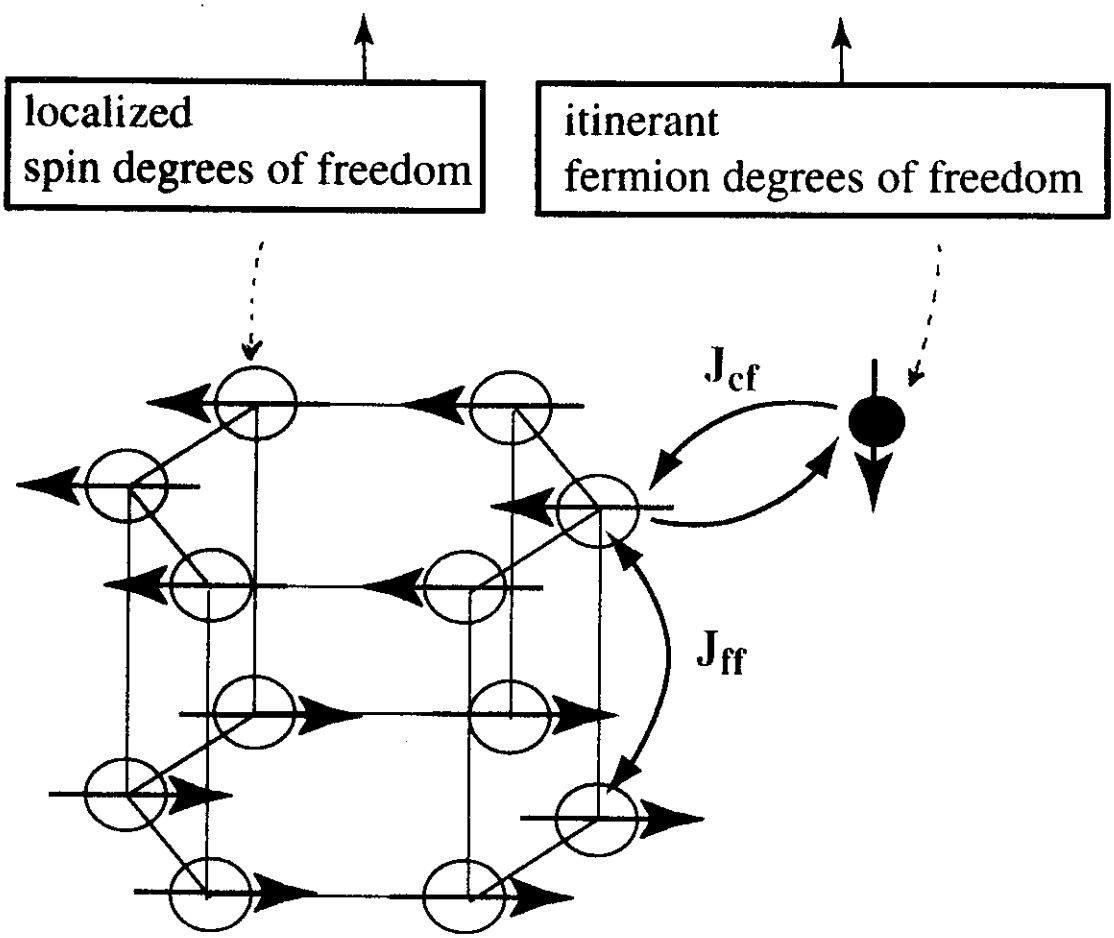


$J_{ff}$ AF order

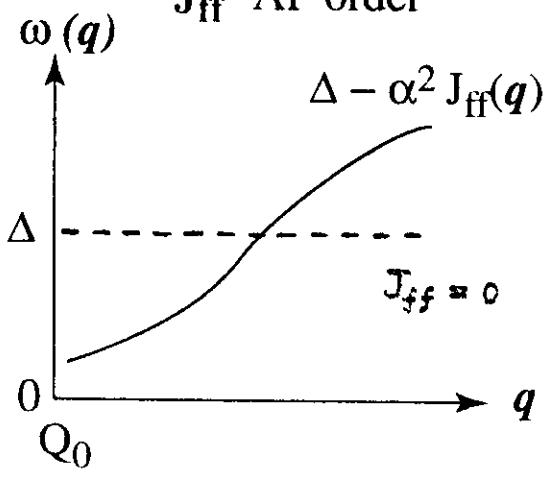


$J_{cf}$ broadening (and shift)

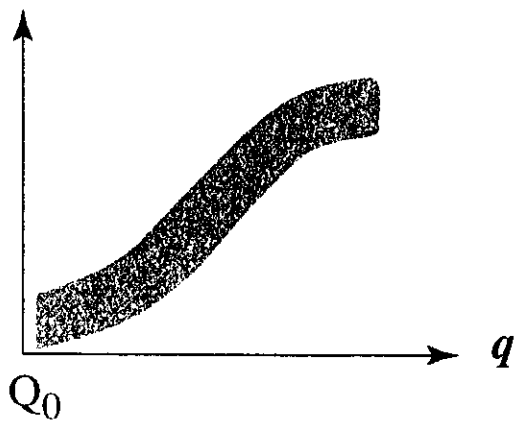

eq. of motion

$$G_{ff} = g_f - g_f J_{ff} G_{ff} - g_f J_{fc} G_{cf}$$

$$G_{cf} = -g_c J_{cf} G_{ff}$$

$\frac{d^2\sigma}{d\omega d\Omega} \propto \mathrm{Im}\, G_{ff}$

**Localized component**

$$g_f = \frac{2\alpha^2}{\omega^2 - \Delta^2} \sim \frac{\alpha^2}{\omega - \Delta} \qquad ; \alpha = \langle \Gamma_5 | J_+ | \Gamma_4 \rangle$$

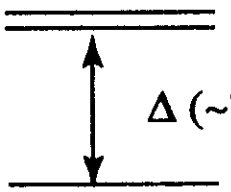

$\Gamma_5 = 0.96\,|\mp 2\rangle - 0.26\,|\pm 4\rangle$

$\Delta$ (~7meV)

$\Gamma_4 = 1/\sqrt{2}\,(|3\rangle - |-3\rangle)$ → magnetic exciton

$\Delta \sim 7$ meV, $J_{ff}(\vec{q} = \vec{Q}_0) \sim 0.7$ meV → $T_N \sim 25$ K, $\mu_S \sim 0.6\,\mu_B$

**Itinerant component**

$$g_c = \chi(q)\left[1 - \frac{\omega\,(\omega + i\,\Gamma(q))}{\omega_{SC}^2 - i\,\Gamma(q)\,(\omega + i\,\Gamma(q))}\right]^{-1} \qquad T \lesssim T_C$$

$$\xrightarrow[\omega_{SC} \to 0]{} \frac{\chi(q)}{1 - i\,\omega / \Gamma(q)} \qquad T \gtrsim T_C$$

$(\omega_{SC} = 2\Delta_{SC})$

$$G_{ff} = g_f - g_f J_{ff} G_{ff} + g_f J_{fc} g_c J_{cf} G_{ff}$$

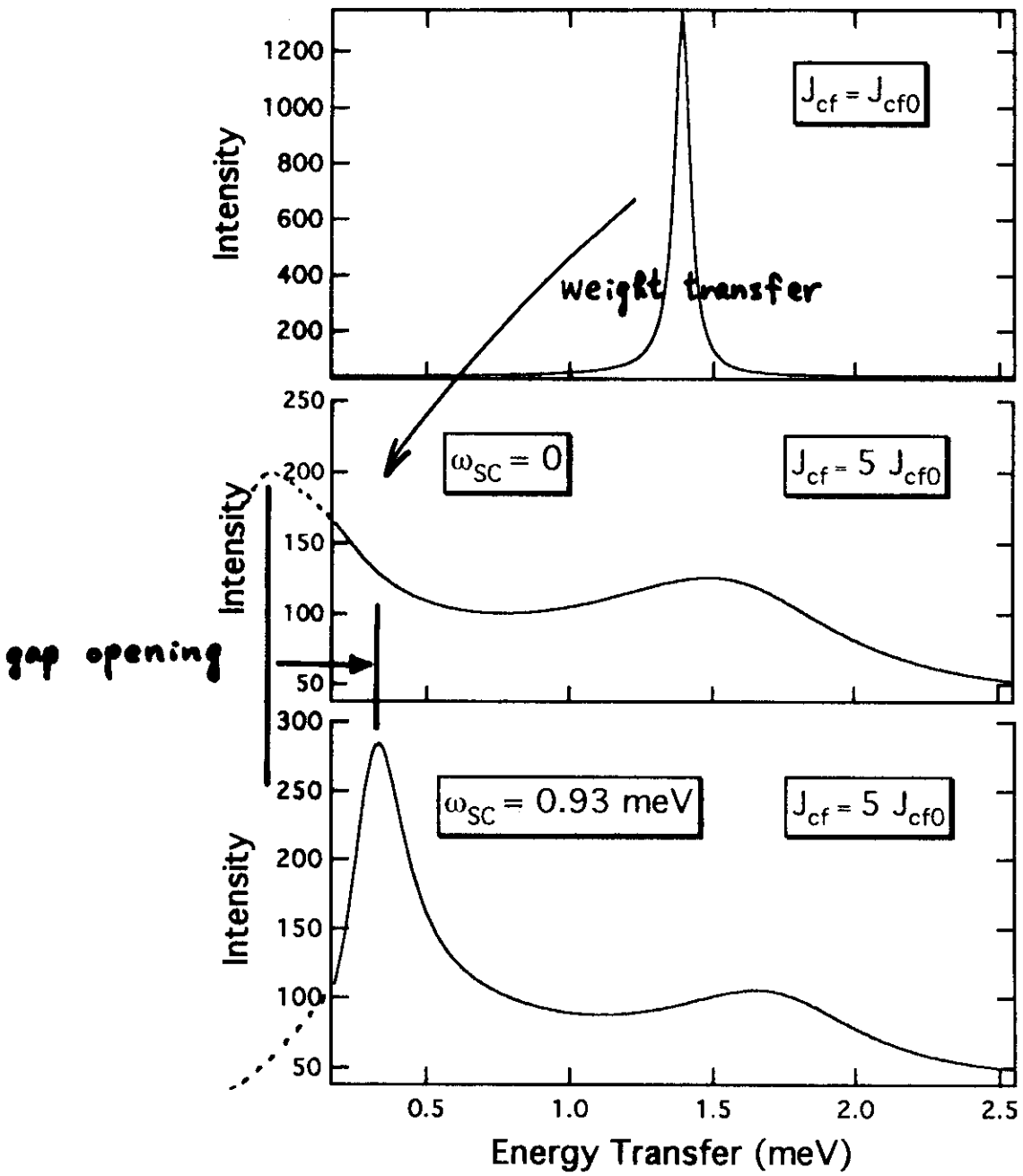

$\omega_{SC} = 6\ k_B T_c$

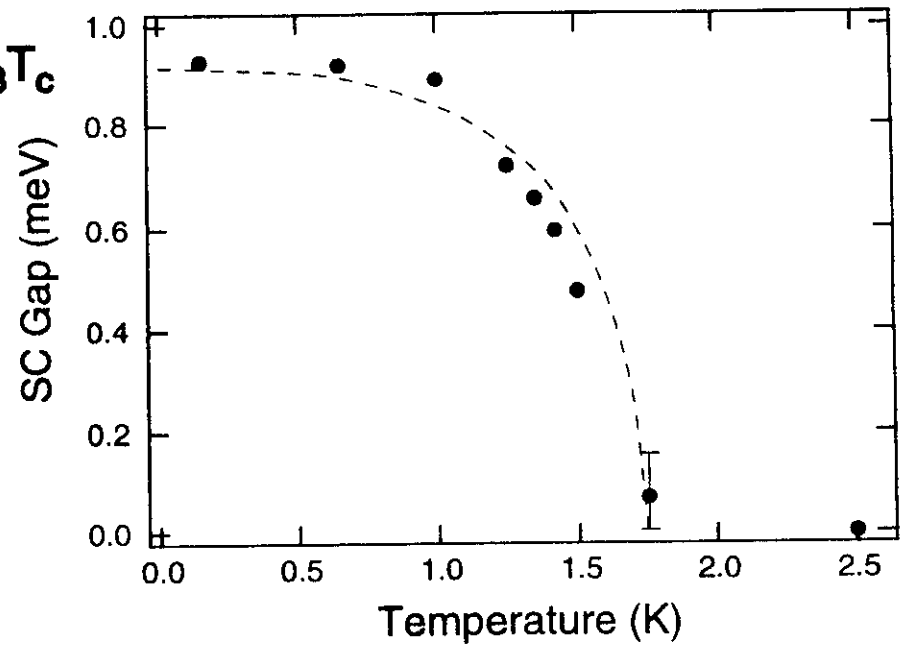


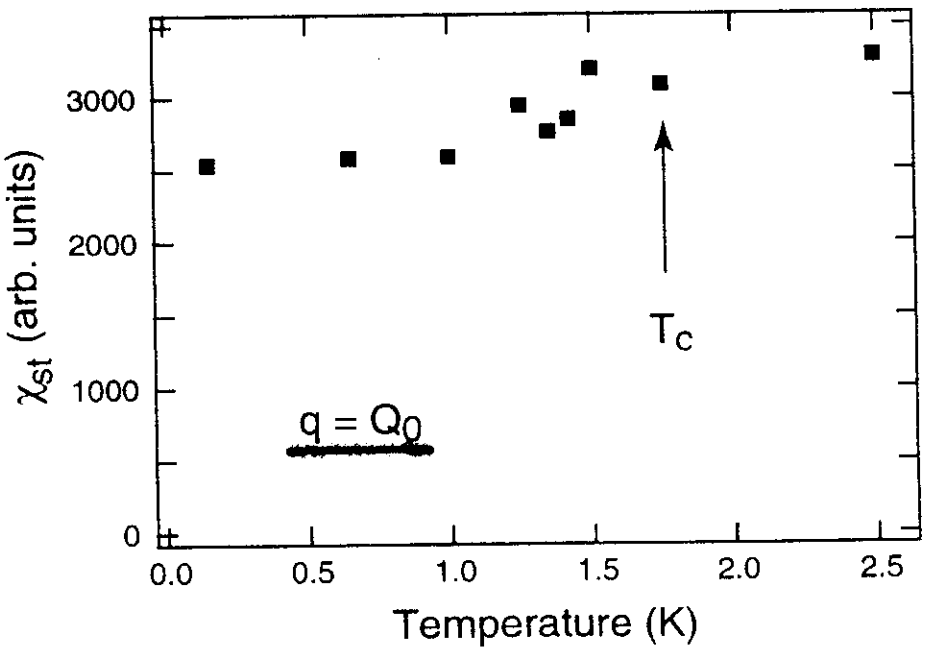

# Superconductivity mediated by spin fluctuations in the heavy-fermion compound $UPd_2Al_3$

**M. Jourdan, M. Huth & H. Adrian**
*Institute of Physics, Johannes Gutenberg-University, Staudingerweg 7, 55099 Mainz, Germany*

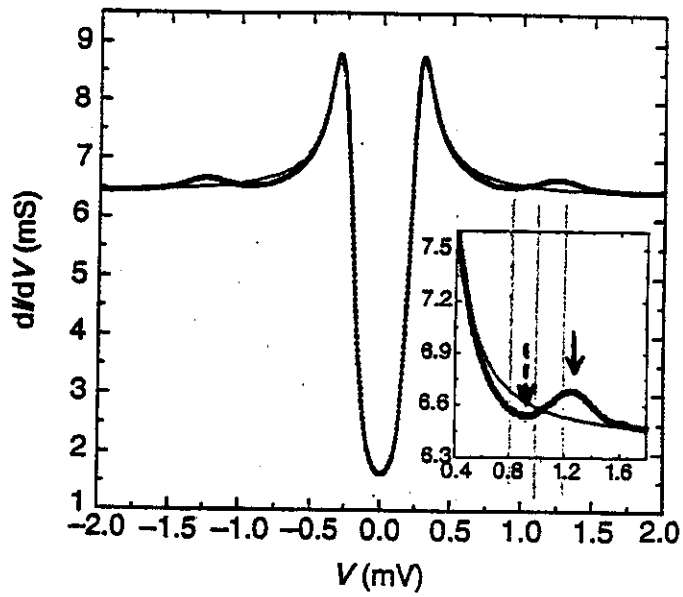


**Figure 4** Normalized differential conductivity of a $UPd_2Al_3$–$AlO_x$–Pb tunnel junction. Black trace, experimental results for $T = 0.3$ K, $B = 0.3$ T; grey trace, fit to the Dynes formula with $\Delta = 235\ \mu$eV, $\Gamma = 35\ \mu$eV (see text). Inset, spin-fluctuation strong-coupling structures of $UPd_2Al_3$ (same axis parameters as main plot).

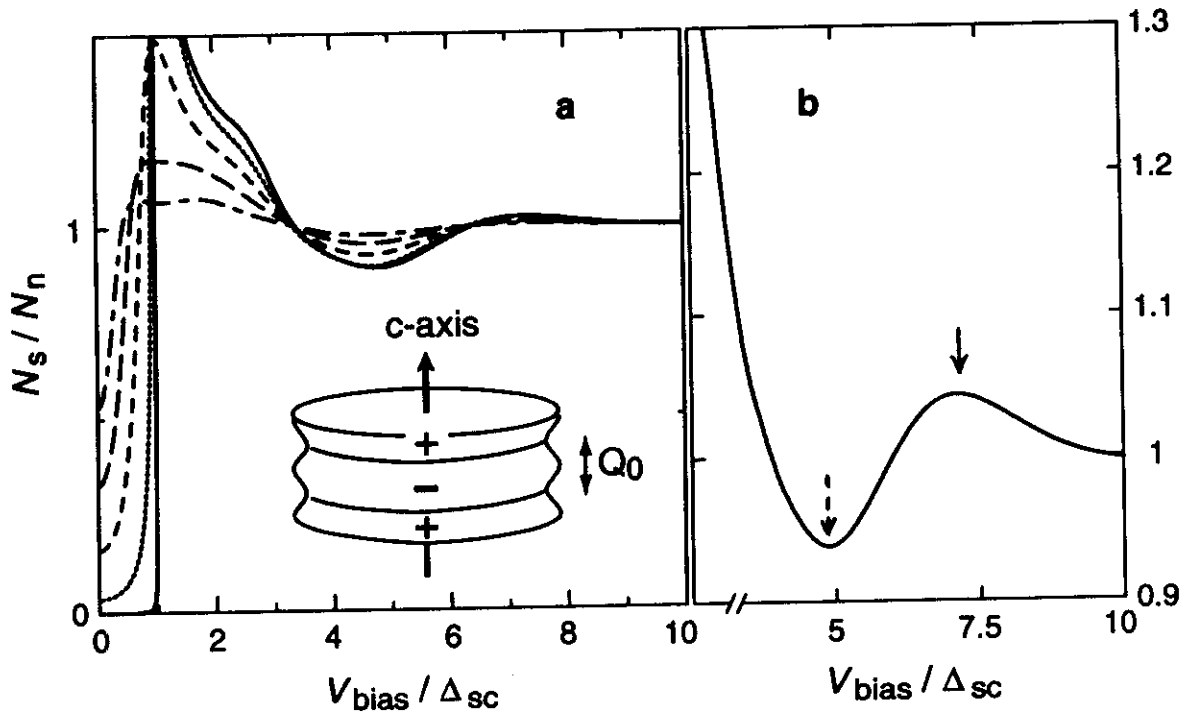


Calculation

$2\Delta_{sc}/k_B T_c \simeq 5.6$

N.K. Sato et al. Fig.3

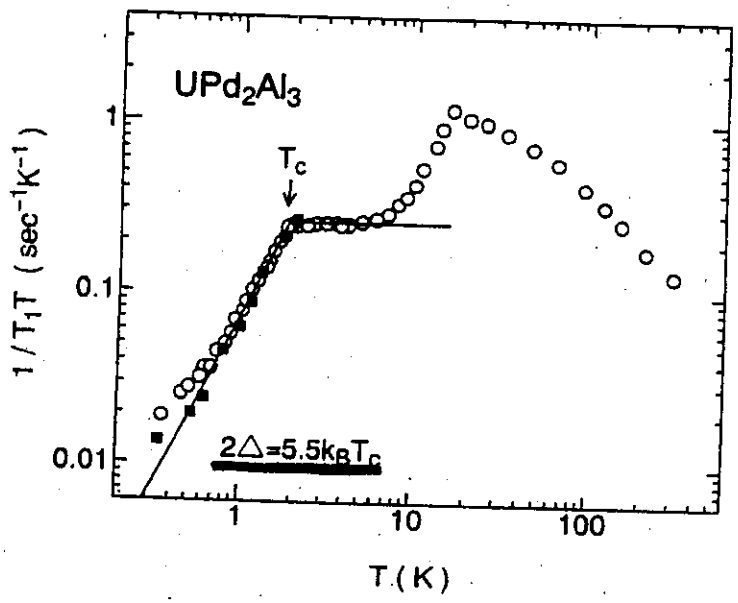


Fig. 14. Temperature dependence of $^{27}(1/T_1T)$ in $UPd_2Al_3$ for $H \perp c$ at $H=2.8$ kOe (■) and 4.9 kOe (○). Solid line is calculated on the anisotropic energy gap model with line of gap zeros at the Fermi surface, $\Delta(\theta)=\Delta \cos(\theta)$ with $2\Delta=5.5\, k_B T_c$.[5]

( Kyogaku et al.)

Miyake & N.K.S.

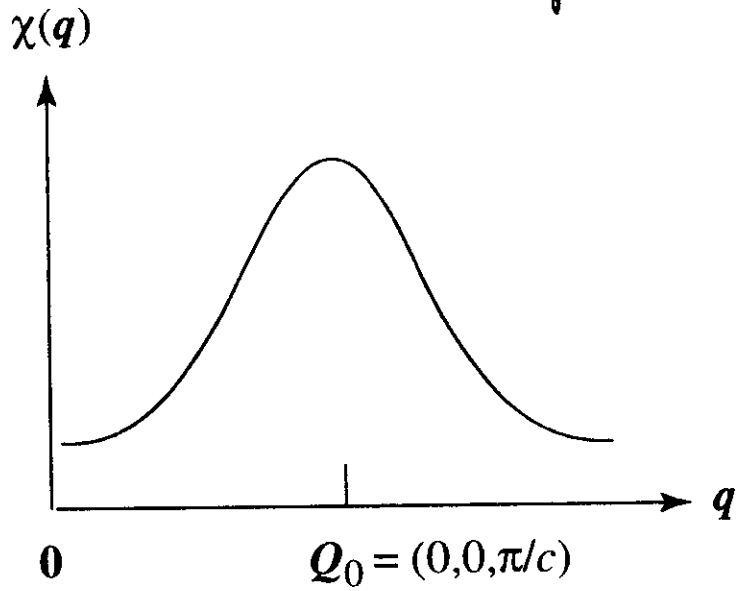


strength of pairing interaction for the singlet channel

$$-3\,V_{k,k'} = 3\,\lambda^2\,\chi(k-k',0)$$

coupling between itinerant and localized component

$$\Delta(k) = \Delta_0 + \Sigma_n\,\Delta_n \cos[(2n-1)k_z c]$$
$$\sim \Delta_1 \cos(k_z c) \qquad (\Delta_0 \ll \Delta_1)$$

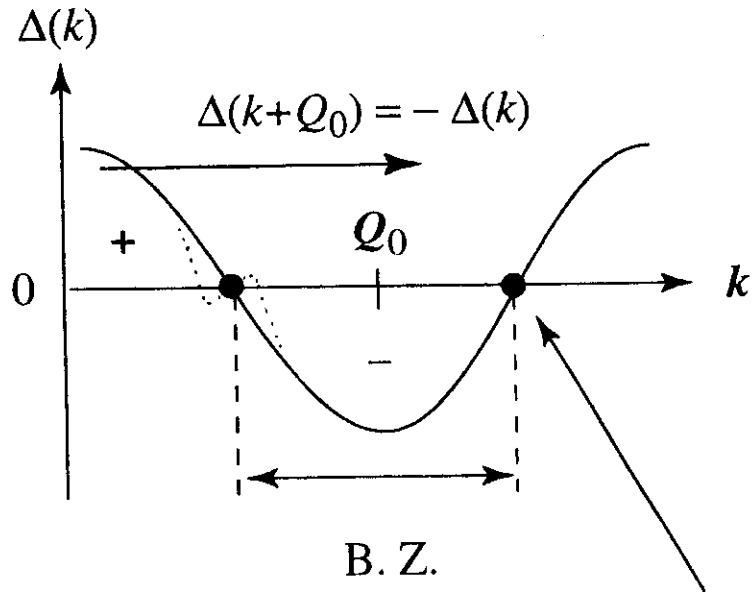


**gap node near the zone boundary**

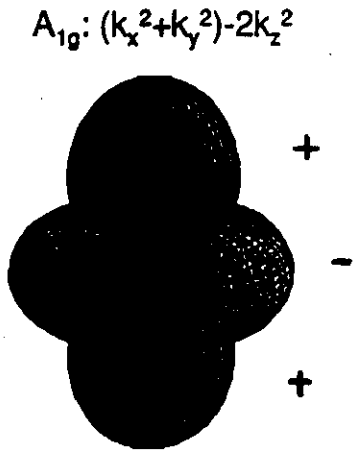


Figure 6.6: *Even parity basis functions for point group symmetry $D_{6h}$. The absolute value of the basis functions, which represent the angular dependence of the energy gaps are plotted on a Fermi sphere in analogy to the two-dimensional representation in Fig. 1.1. The sign of the phase of the order parameter is changing at every line node.*

line nodes



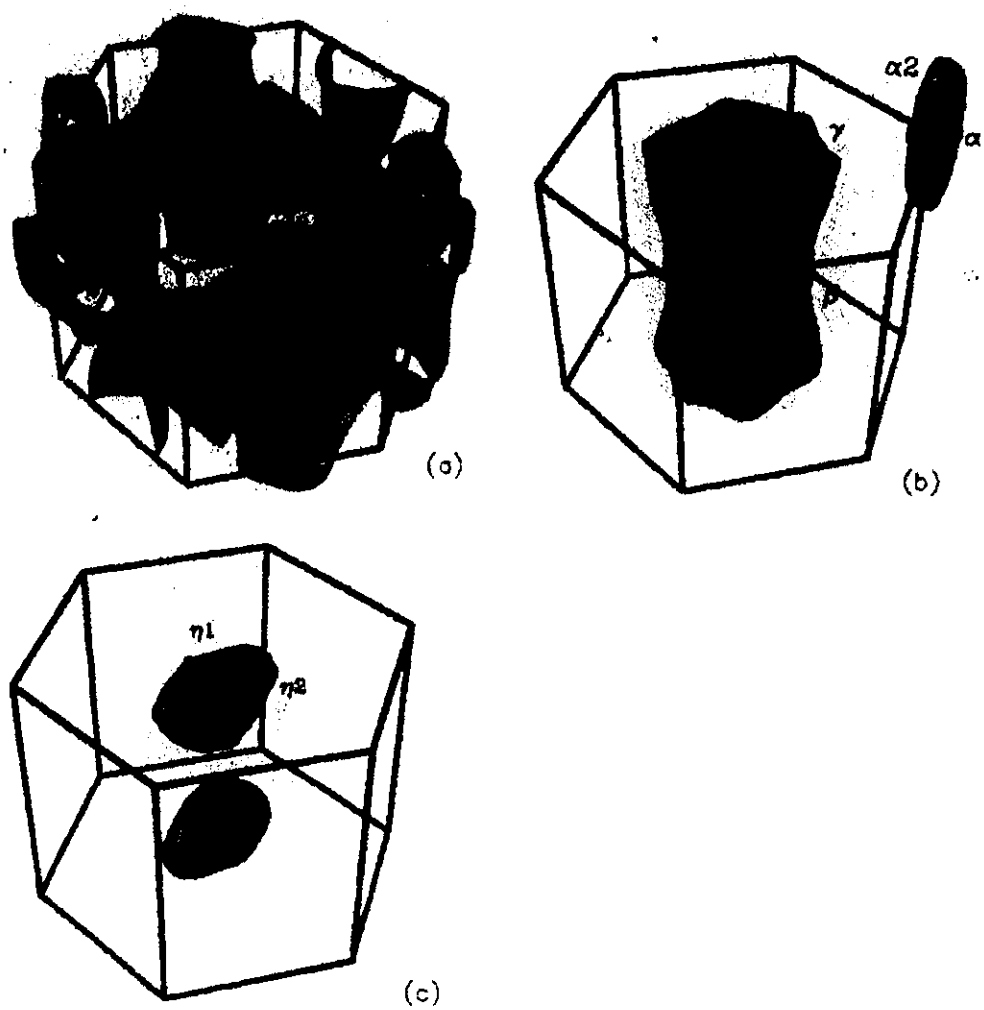


**Figure 5.** Definitions of the various extremal orbits employed in figure 4: (a) the 'party hat'; (b) the 'column' and 'cigars'; (c) the 'egg'.

BCS superconductivity

$$T_c \sim T_D e^{-1/N(0)V}$$

Spin fluctuation mediated superconductivity

$$T_c \propto \underline{T_0} \quad ; \text{ Moriya et al.}$$

$$\chi(q,\omega) = \frac{\chi(q)}{1 - i\omega/\Gamma(q)}$$

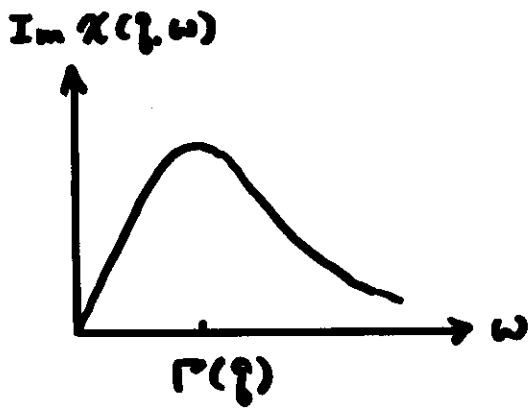


$$\Gamma(q) \propto \Gamma\,(q^2 + \kappa^2)$$

$$= 2\pi \underline{T_0}\,(q^2 + \kappa^2)/q_B^2$$

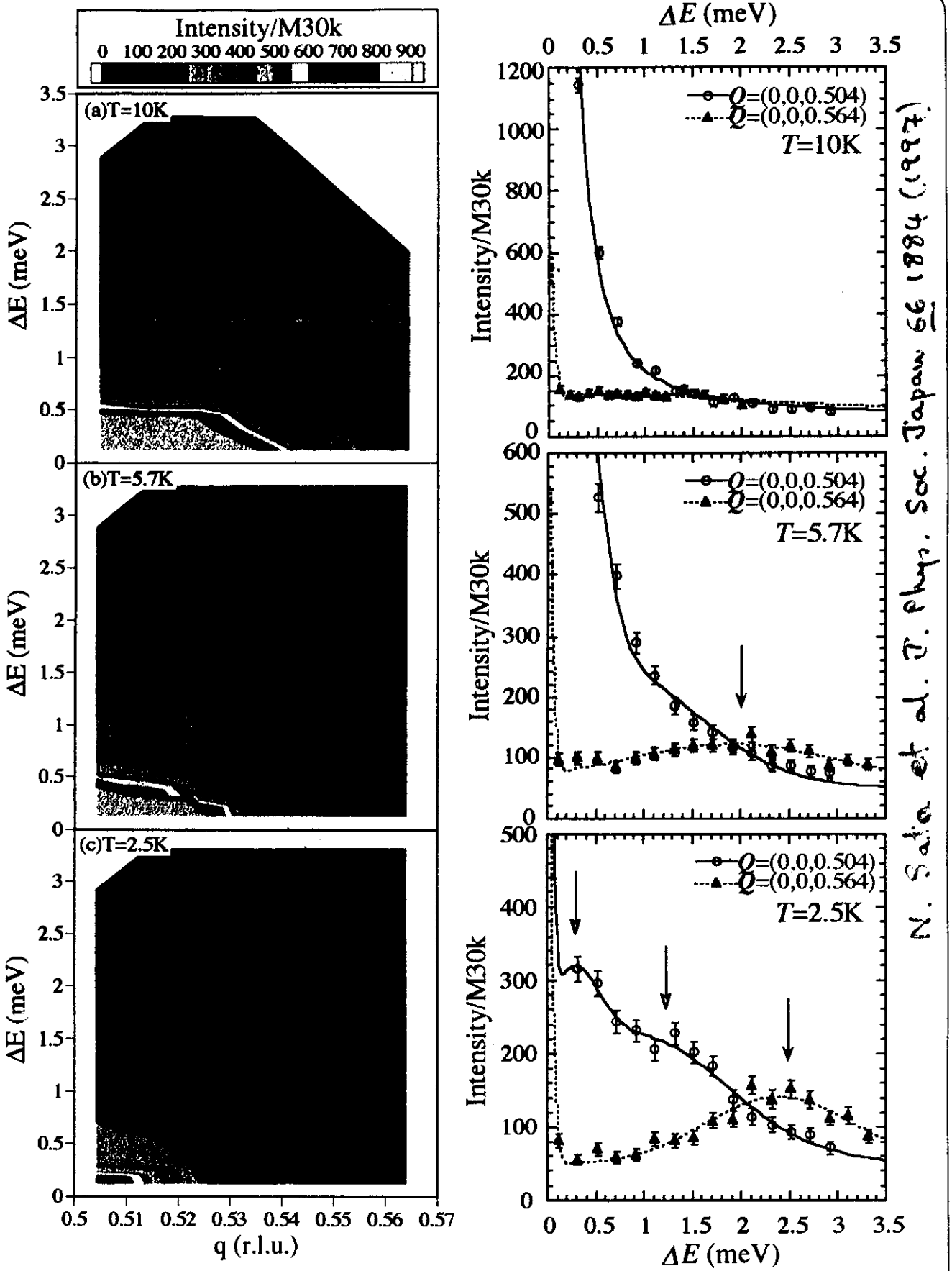


(a)T=10K、(b)T=5.7K、(c)T=2.5Kでの生データのContourMap（左図）と各温度における$\boldsymbol{Q}$=(0,0,0.504)、$\boldsymbol{Q}$=(0,0,0.564)のコンスタント$\boldsymbol{Q}$スキャン。

$$\chi(\vec{q},\omega,T) = \frac{\chi(\vec{q},T)}{1 - i\frac{\omega}{\Gamma(\vec{q},T)}}$$

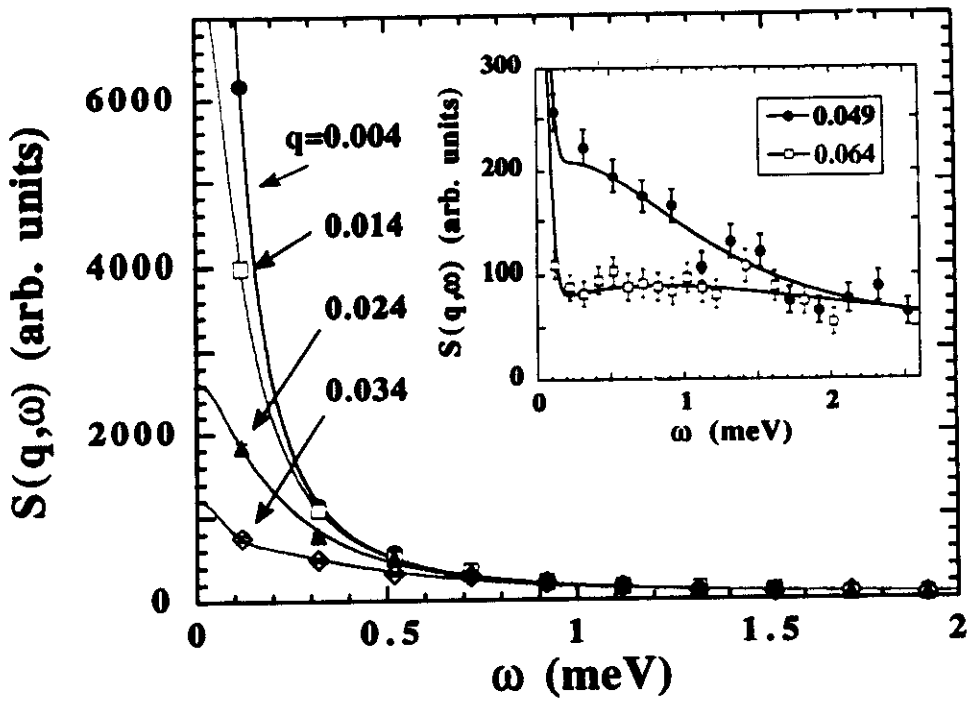


T = 10 K

$$\frac{1}{\chi(\vec{q},T)} \approx \frac{1}{\chi(\vec{q}=\vec{0},T)} + A\vec{q}^2 = 2T_A\left[\left(\frac{K}{q_D}\right)^2 + \left(\frac{q}{q_D}\right)^2\right]$$

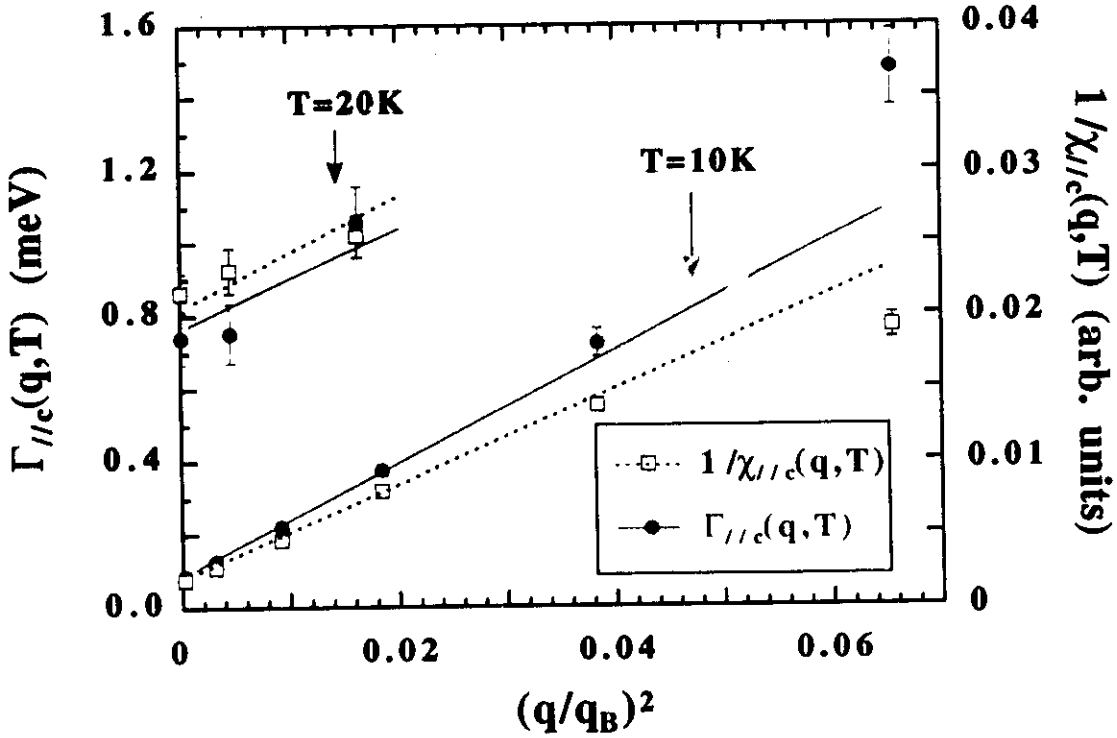


$$\Gamma(\vec{q},T) \approx \Gamma(\kappa^2 + q^2) = 2\pi T_0\left[\left(\frac{K}{q_D}\right)^2 + \left(\frac{q}{q_D}\right)^2\right]$$

$T_0 = \begin{cases} 2.5 \text{ meV at } 10\text{ K} \\ 2.2 \text{ meV at } 20\text{ K} \end{cases}$

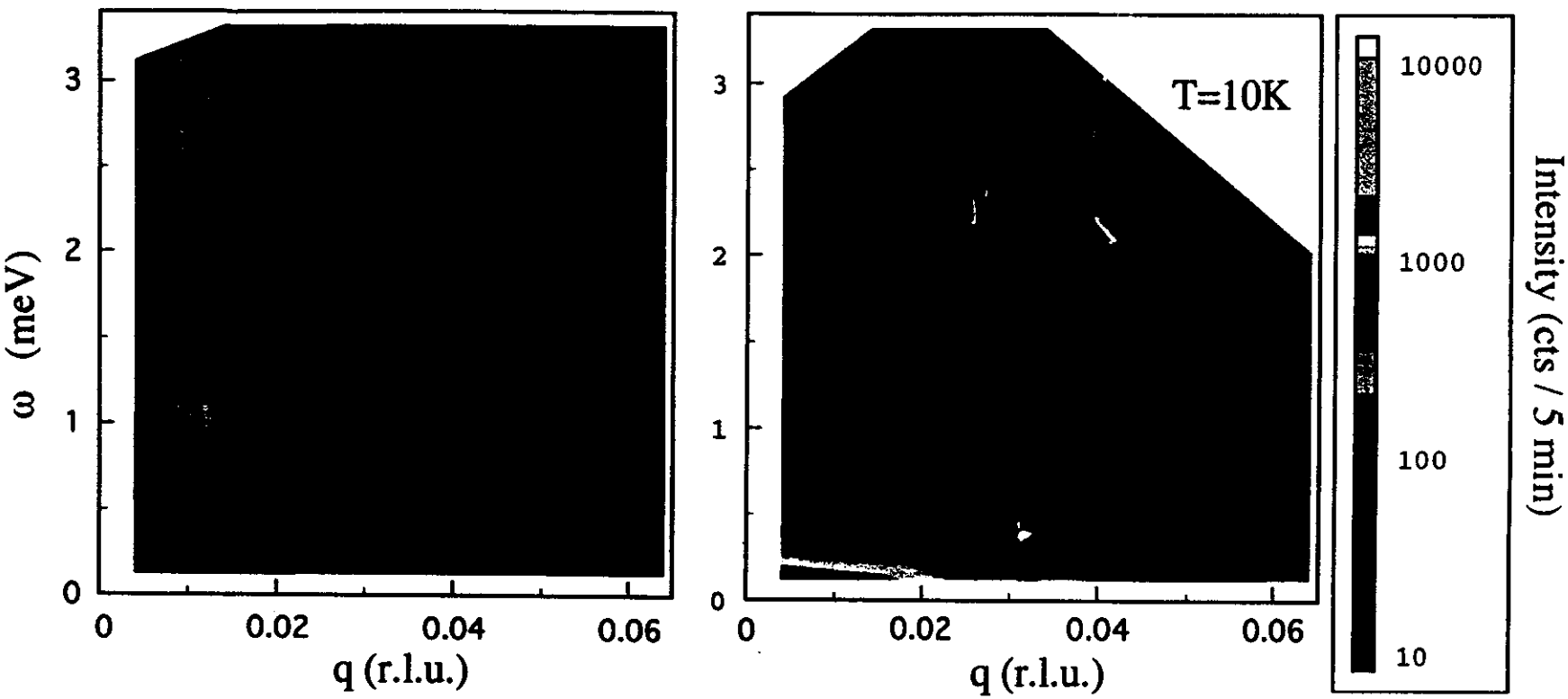


J. P. S. J. 66 ('97) 1884.

Fig.1

**Itinerant component**

$$g_c = \chi(q) \left[ 1 - \frac{\omega\,(\omega + i\,\Gamma(q))}{(2\Delta_{SC})^2 - i\,\Gamma(q)\,(\omega + i\,\Gamma(q))} \right]^{-1} \qquad T \ll T_C$$

$$\xrightarrow[\Delta_{SC} \to 0]{} \frac{\chi(q)}{1 - i\,\omega / \Gamma(q)} \qquad T \gg T_C$$

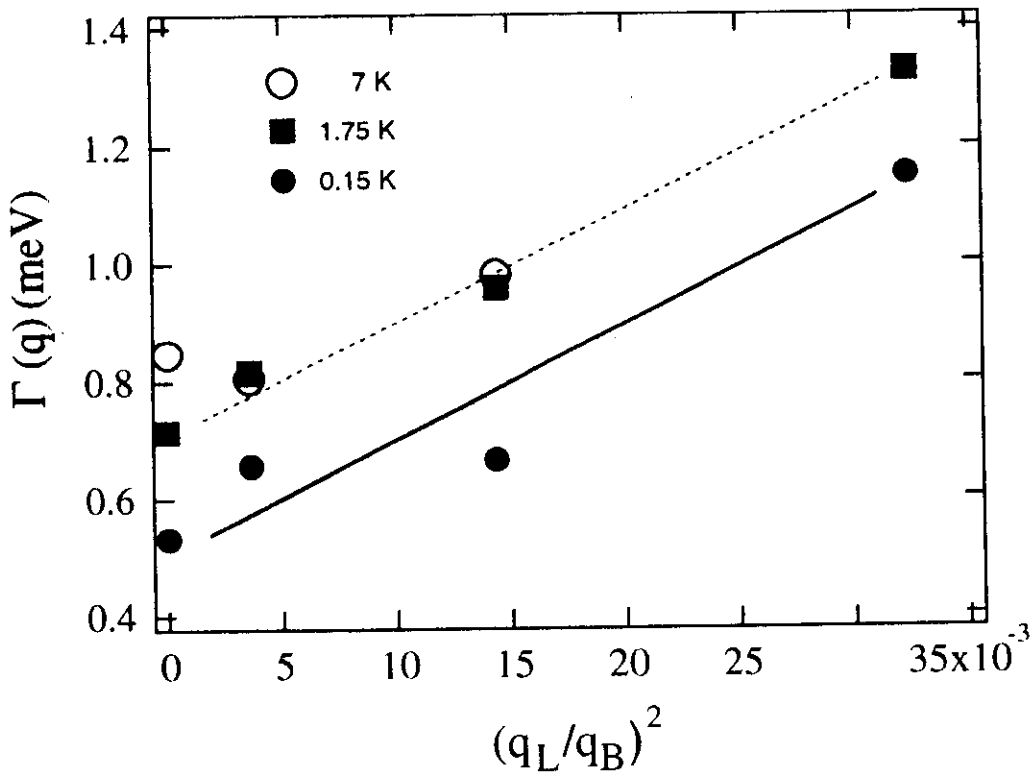


$$\Gamma(q) = \Gamma\,(\kappa^2 + q^2)$$

$$= 2\pi T_0\,((\kappa/q_B)^2 + (q/q_B)^2)$$

$T_0 \sim 34$ K

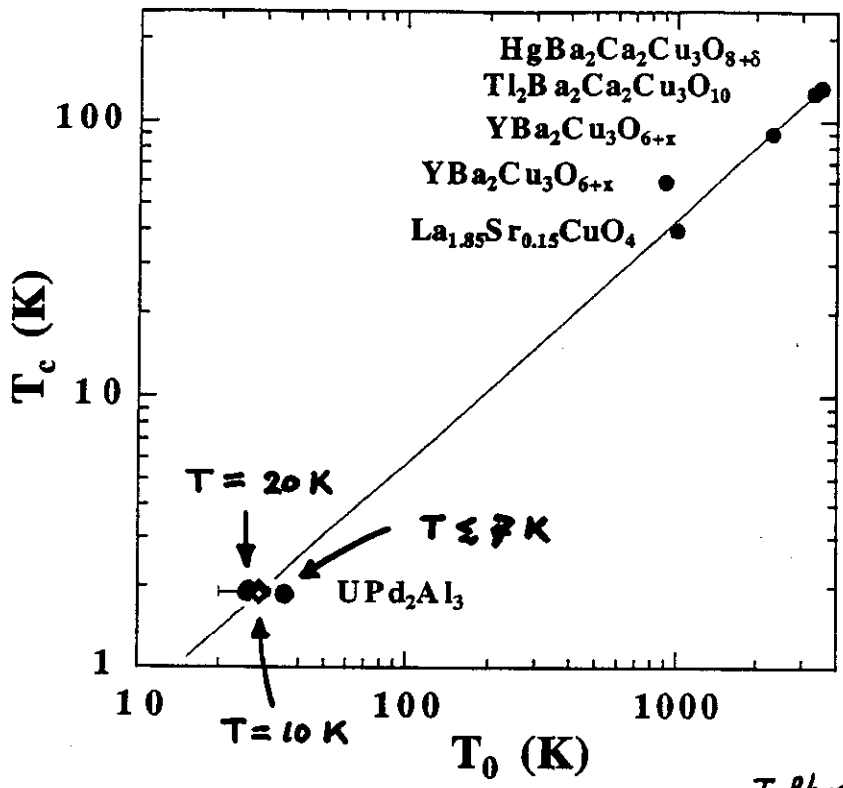


J. Phys. Soc. Jpn. 66 (97) 1884

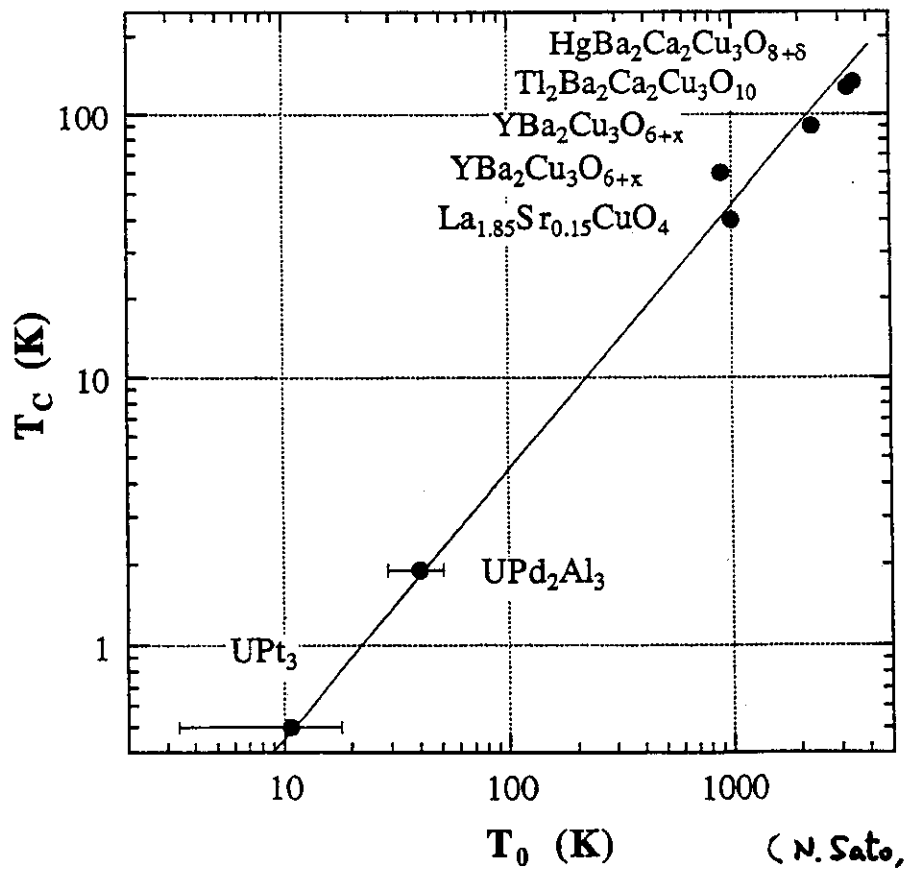


(N. Sato, SCES Paris)

# Neutron-scattering study of the magnetic response in the heavy-fermion superconductor $UNi_2Al_3$

N. Aso*
*Department of Physics, Graduate School of Science, Tohoku University, Sendai 980-8578, Japan*

B. Roessli
*Laboratory for Neutron Scattering, ETH Zurich and Paul Scherrer Institute, CH-5232 Villigen, Switzerland*

N. Bernhoeft and R. Calemczuk
*Département de Recherche Fondamentale sur la Matière Condensée, Commissariat à l'Énergie Atomique-Grenoble, F-38054 Grenoble, France*

N. K. Sato,† Y. Endoh, and T. Komatsubara
*Department of Physics, Graduate School of Science, Tohoku University, Sendai 980-8578, Japan*

A. Hiess
*Institut Laue Langevin, BP 156X, F-38042 Grenoble, France*

G. H. Lander
*European Commission, Joint Research Centre, Institute for Transuranium Elements, Postfach 2340, D-76125 Karlsruhe, Germany*

H. Kadowaki
*Department of Physics, Tokyo Metropolitan University, Hachioji, Tokyo 192-0397, Japan*
(Received 28 February 2000)

High-resolution neutron inelastic scattering has been used to probe the magnetic response in the heavy-fermion superconductor $UNi_2Al_3$. Quasielastic scattering has been observed both below and above $T_c$ in the vicinity of the incommensurate magnetic ordering vector $\mathbf{Q}_0=(0.39, 0, 0.5)$. Features in the response are similar to those reported recently for the isostructural compound $UPd_2Al_3$. However, in contrast to the situation in $UPd_2Al_3$, no spectral gap has been observed in the dynamical susceptibility of $UNi_2Al_3$, even at the lowest temperature of 0.2 K.

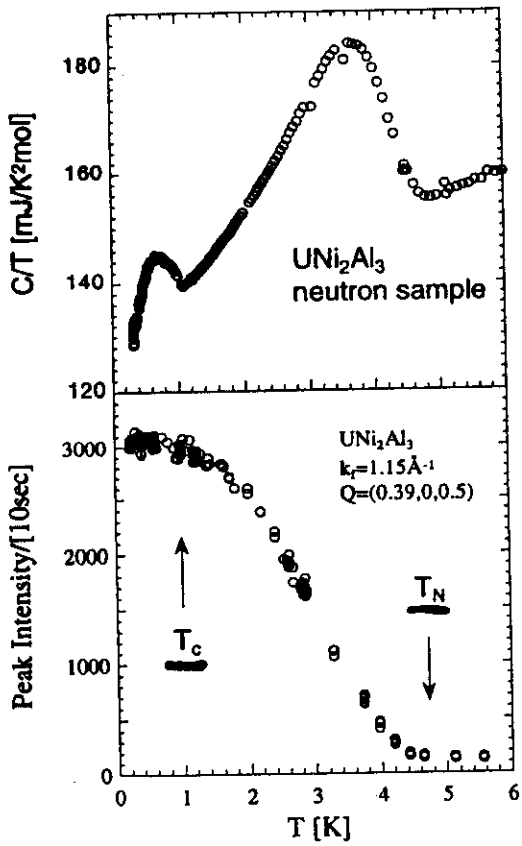


FIG. 1. Upper panel: Temperature dependence of the ratio $C/T$ as measured on the crystal used in the neutron experiments. Lower panel: Temperature dependence of the peak intensity at the antiferromagnetic Bragg peak $\mathbf{Q}_o=(0.39, 0, 0.5)$. The arrows mark the Néel ($T_N$) and superconducting ($T_c$) temperatures.

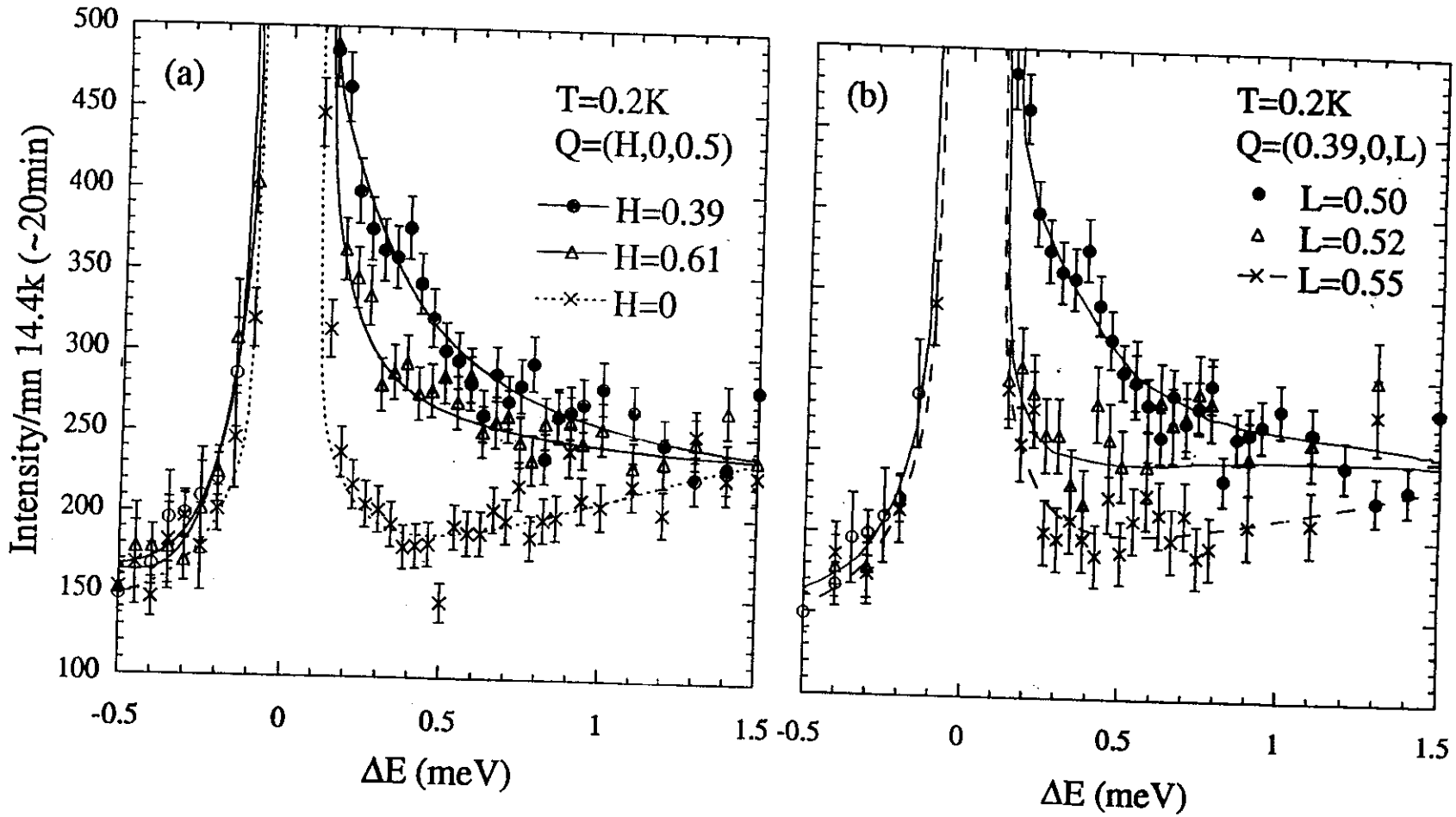


N. Aso et al. Fig. 2.

# Summary

**quasiparticles**

**itinerant part of 5*f* electrons**

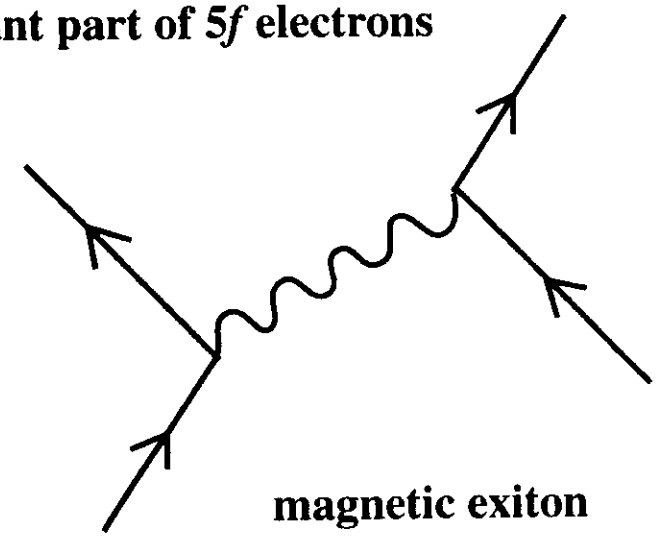

**magnetic exiton**

**localized part of 5*f* electrons**

**Localized moments mediate SC pairing interacton.**

(quasi-one-component?)

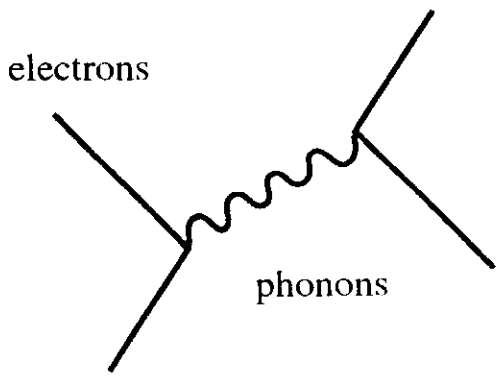


two component

conventional superconductor

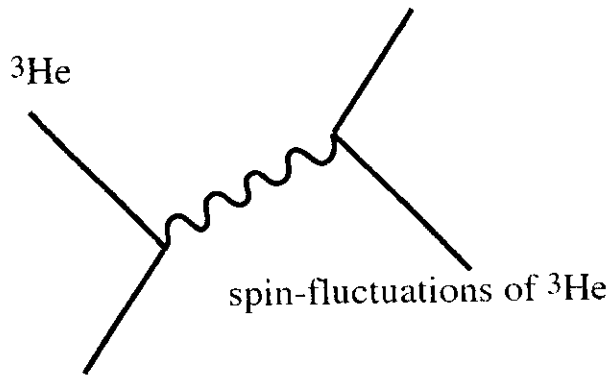


one component

liquid $^3$He
High $T_c$ cuprates ?